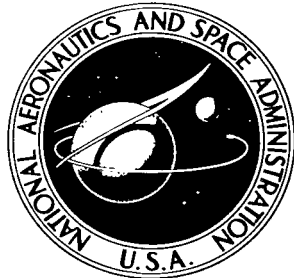


NASA TN D-3324

NASA TECHNICAL NOTE



NASA TN D-3324

0.1

1 QAN COPY; RETURN
AFWL (WVH-2)
17 APR 1966

0079972



TECH LIBRARY KAFB, NM

THEORETICAL BACKGROUND FOR THERMIONIC
CONVERSION INCLUDING SPACE-CHARGE THEORY,
SCHOTTKY THEORY, AND THE ISOTHERMAL
DIODE SHEATH THEORY

by

Wayne B. Nottingham

Massachusetts Institute of Technology

Cambridge, Mass.

and

Roland Breitwieser

Lewis Research Center

Cleveland, Ohio

NATIONAL AERONAUTICS AND SPACE ADMINISTRATION • WASHINGTON, D. C. • MARCH 1966





0079972

NASA TN D-3324

**THEORETICAL BACKGROUND FOR THERMIONIC CONVERSION
INCLUDING SPACE-CHARGE THEORY, SCHOTTKY THEORY,
AND THE ISOTHERMAL DIODE SHEATH THEORY**

By Wayne B. Nottingham

**Massachusetts Institute of Technology
Cambridge, Mass.**

and Roland Breitwieser

**Lewis Research Center
Cleveland, Ohio**

NATIONAL AERONAUTICS AND SPACE ADMINISTRATION

**For sale by the Clearinghouse for Federal Scientific and Technical Information
Springfield, Virginia 22151 — Price \$0.70**

CONTENTS

Section	Title	Page
I	INTRODUCTION	1
II	GENERAL DESCRIPTION OF SPACE-CHARGE PROBLEM	2
III	LANGMUIR SPACE-CHARGE EQUATION	5
IV	ANALYTICAL DEVELOPMENT OF SPACE-CHARGE RELATIONS	10
V	APPLICATION OF MASTER CURVE	16
VI	TRANSITION CURVES IN SPACE-CHARGE REGION	17
VII	LIMITING SPACE-CHARGE CURVE	20
VIII	REMARKS CONCERNING APPLICATION OF SPACE-CHARGE THEORY	21
IX	GENERAL DISCUSSION OF SCHOTTKY MIRROR-IMAGE THEORY	22
X	CONCLUDING REMARKS CONCERNING USE OF SCHOTTKY THEORY	26
XI	REVIEW OF SHEATH AND PLASMA THEORY OF ISOTHERMAL DIODE	27
XII	FOWLER POTENTIAL FUNCTION IN SHEATH	29
XIII	RELATION OF ISOTHERMAL DIODE THEORY TO SCHOTTKY REDUCTION IN WORK FUNCTION	32
XIV	CONCLUDING REMARKS CONCERNING ISOTHERMAL DIODE THEORY	33
XV	ADDITIONAL AIDS TO ANALYSIS OF THERMIIONIC CONVERTER PERFORMANCE	34
XVI	CONCLUDING REMARKS	41
XVII	SYMBOLS	41
XVIII	REFERENCES	44

THEORETICAL BACKGROUND FOR THERMIONIC CONVERSION
INCLUDING SPACE-CHARGE THEORY, SCHOTTKY THEORY,
AND THE ISOTHERMAL DIODE SHEATH THEORY
by Wayne B. Nottingham* and Roland Breitwieser
Lewis Research Center

SUMMARY

A theoretical background to the analysis of thermionic converter performance is presented. The areas of theory treated include (1) space-charge theory for the case where either electrons or ions are the predominant charge carriers, (2) Schottky mirror image theory for ion and electron emission, and (3) Fowler theory applied to a plasma in equilibrium with an emitting surface, treated in terms of the relation of the plasma potential to surface potentials and in terms of the character of the sheath. Included are various graphical and tabulated aids to the analysis of cesium filled thermionic converters. Simplicity of theory and assumption is emphasized so as to yield convenient analytical tools for the first order examination and treatment of thermionic converter data.

I. - INTRODUCTION

Stimulated by the need for an energy conversion system that minimizes the weight per kilowatt, the direct conversion of heat to electricity by thermionics has been intensively investigated in many research centers for the past several years. As a part of this effort many excellent detailed analyses and experimental studies of thermionic processes have been developed. Experience has shown that knowledge of space-charge, Schottky, Fowler (sheath), and isothermal diode theories are required for many phases of this thermionic converter research. A series of lectures by the authors covering these analytical areas has been combined and is the framework of this report.

Space-charge theory is reviewed for the case where the charge carrier is predominantly of one sign. This theory applies directly to the vacuum diode and often can be extended to the analysis of the performance of the plasma diode. The Schottky theory of the transmission of electrons in strongly accelerating fields is reviewed, and simplified relations are developed. A brief review of the theory of the isothermal diode and guides to its application are presented. Reference is made to the Fowler space-charge theory in the isothermal diode analysis. The Fowler theory is used to describe the potential variation of the plasma sheath between the conductor surface and the isothermal plasma.

The primary intent of this report is to translate these well-known theoretical developments into a form amenable to treating experimental data. Review and, on occasions, modified development of theory have been included so that the limitations of theory are thus established. It is felt that the analytical approaches suggested can serve as important aids to the understanding of practical

*Massachusetts Institute of Technology, deceased, 1964.

thermionic converters despite the fact that experimental conditions seldom fit the specific boundary conditions set by theory.

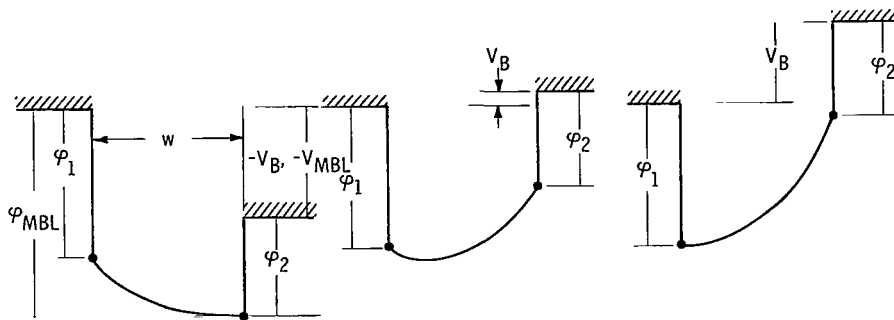
II. - GENERAL DESCRIPTION OF SPACE-CHARGE PROBLEM

The equations to be summarized in this section apply to either electron or ion emission across a diode. The initial formulation relates to the current-voltage curve that describes the delivery of electrons to a collector in absence of any ions. The analysis assumes the emitter and collector work functions are uniform, the surfaces are parallel, infinite planar areas exist, and the temperatures are known. The various ranges of interest are shown in the electron potential diagrams (figs. II:1(a) to (c)) and the corresponding current-voltage curve (fig. II:1(d)). Figure II:1(b) is a typical potential diagram in the space-charge range. Figures II:1(a) and (b) represent the potential distribution at the limits of the space-charge range. The electron potential diagram of special importance is shown in figure II:1(a) in which the interelectrode potential merges with collector potential with zero slope. This is a critical condition of zero field at the collector and serves to separate the "space-charge range" from the "Boltzmann range" and is identified as the Maxwell-Boltzmann limit (MBL). The applied potential at this Maxwell-Boltzmann limit is identified by V_{MBL} . The collector work function φ_2 is defined as the difference between the collector Fermi level and surface potential. Thus, the surface potential φ_{MBL} relative to the emitter Fermi level is equal to absolute sum of the applied potential V_{MBL} and φ_2 . Over the range of voltage more negative than this limiting value V_{MBL} , the current observed is a direct measure of the total outflow of electrons from the emitter that have a sufficient energy to overcome the surface barrier at the collector. The straight line portion of the logarithm of the current plotted against voltage is this Boltzmann range (fig. II:1(d)). The equation that relates this current to the applied voltage is the following form of the Richardson-Dushman emission equation:

$$-J_B = 120 \times 10^4 T^2 \exp\left[\frac{-q(\varphi_2 - V_B)}{kT}\right] \text{ amp/sq m} \quad (\text{II:1})$$

The equation is written in its general form. The sign convention used is as follows: the work function φ is always treated as a positive quantity. When the Fermi level of the collector is negative with respect to the emitter (displaced downward in fig. II:1(a)), the applied voltage V_B is negative and cancels the negative sign in the parenthesis in equation (II:1). The quantity $(\varphi_2 - V_B)$ represents the surface barrier at the collector that suppresses electron flow from the emitter and is therefore referenced to the emitter Fermi level. It follows that at a given emitter temperature, φ_2 can be determined directly from the current density $-J_B$ and applied voltage V_B . The emitter temperature may also be obtained from the straight line portion of the logarithm of current of a plot such as figure II:1(d). Noting that T appears in the exponent in equation (II:1), it then follows directly that emitter temperature can be established at any arbitrary current ratio

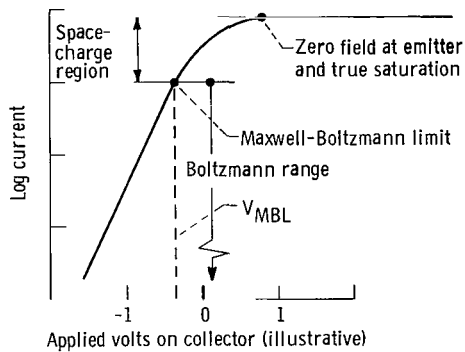
$$T = \frac{(V_{B,2} - V_{B,1}) \ln 606}{\ln\left(\frac{-J_{B,2}}{-J_{B,1}}\right)} \text{ } ^\circ\text{K} \quad (\text{II:2})$$



(a) Typical potential at Maxwell-Boltzmann limit (start of space-charge region V_B is equal to to V_{MBL} ; if voltage is more negative, Boltzmann range is entered).

(b) Example of potential in space-charge region.

(c) Example of potential with zero field at emitter (corresponds to saturation current condition).



(d) Current-voltage curve.

Figure II:1. - Ranges of interest in space-charge analysis of planar diode.

Various current ratios may be used. For example, a convenient current ratio of 3.197 results in

$$T = (V_{B,2} - V_{B,1})10^4 \quad ^\circ\text{K} \quad (\text{II:3})$$

As the applied voltage V_B is changed to make the surface potential less negative, the linear portion of the logarithmic current-voltage curve terminates (fig. II:1(a)). This is the aforementioned critical condition of the limit of the Maxwell-Boltzmann range and the onset of the space-charge condition. At still smaller negative surface potentials, the space-charge minimum moves toward the emitter. A typical potential distribution in the space-charge range is shown in figure II:1(b). Here, although the surface potential of the collector is positive with respect to that of the emitter, the current is determined by the space-charge barrier, which is more negative than the emitter surface potential. The limit of the space-charge range is also shown in the diagram and is associated with the zero slope of the potential at the emitter surface (fig. II:1(c)). The saturation emission capability of the emitter can only be

measured at this condition of zero field at the emitter. The observed current (at zero field) can be used to determine the work function of the emitter by the standard form of the Richardson-Dushman equation

$$-J_0 = 1.2 \times 10^6 T^2 \exp\left(\frac{-q\phi_1}{kT}\right) \text{ amp/sq m} \quad (\text{II:4})$$

Space-charge theory applies specifically to the range of applied voltage for which the surface potential of the collector is varied between that of the Maxwell-Boltzmann limit and that of zero field at the emitter. The theory may be applied to either ions or electrons if proper recognition of charge, particle mass, and potential is made. A surface potential at the Maxwell-Boltzmann limit depends on the spacing, emitter temperature, and to some extent on the emitter work function. If these quantities are known then the applied potential required to establish zero field at the emitter may be computed. The last point is of particular interest since it applies to the evaluation of ion current production at a heated surface in the presence of an easily ionized gas such as cesium. The space-charge relations are also obviously of value in determining the emitter work function from the identification of zero-field emission current.

Diodes of greatest interest to thermionic conversion must necessarily combine the influence of both electrons and ions. The use of the "unicharge", noncollisional space-charge theory limits the quantitative assessment of the properties of the emitter and the collector surface to data obtained at extremely close spacing. As the spacing increases beyond a few microns, plasma conditions develop and current-voltage characteristics are generated that follow the qualitative features associated with the basic space-charge theory, but current-voltage characteristics have to be associated with an "effective spacing" considerably less than the actual interelectrode spacing.

Data obtained near the Maxwell-Boltzmann limit often are less distorted by plasma effects than data obtained near saturation current condition. Thus, the space-charge theory reviewed here is being adapted to determine (1) emission capability of an emitter, (2) information on limiting barriers other than the surface barrier, and (3) effective spacing, by the method of indexing the solution of the space-charge problem to the Maxwell-Boltzmann limit. The results on barriers and spacings apply to both electrons and ions. The evaluation of the barriers and spacing hopefully should lead to a better understanding of the properties of the conducting plasma in the interelectrode space of practical energy converters.

III - LANGMUIR SPACE-CHARGE EQUATION

Langmuir (ref. 1) and others (refs. 2 to 4) have presented and evaluated the basic differential equations relating emitter temperature, charge-to-particle mass ratio, current flow across a diode to the potential as a function of distance. The space-charge formulation involves Poisson's equation, the Maxwell-Boltzmann distribution function, the Boltzmann relation, and conservation equations. The derivation is given in the aforementioned references so it will not be repeated here. The generalized solution makes use of the dimensionless parameters,

$$\psi = \frac{qV}{kT} \quad (\text{III:1})$$

$$x = \frac{KJ^{1/2}x}{\frac{3}{4}T} \quad (\text{III:2})$$

$$K = \frac{q^{1/2}(2\pi m)^{1/4}}{\sqrt{2}\epsilon_0^{1/2}k^{3/4}} \propto K^{3/4}/\text{amp}^{1/2} \quad (\text{III:3})$$

where K is 6.5×10^5 for electrons or is 1.442×10^7 for singly charged cesium ions. The value of x can be obtained conveniently by a nomographic solution presented in figure III:1.

The basic differential equation (ref. 2, for example) is

$$\frac{d^2\psi}{dx^2} = - \left[1 \pm P(\psi^{1/2}) \right] e^\psi \quad (\text{III:4})$$

where P is the well-known "probability integral". The plus sign in equation (III:4) is used in the emitter region (i.e., the region between the space-charge minimum and the emitter), and the negative sign applies to the collector region. The equation can be integrated once to yield a result suitable for numerical integration. The numerical solutions for both regions are given in table III:1 and are essentially equivalent to the values given in references 2, 4, and 5; the small differences reflect the difference in the numerical computing procedures.

Figure III:2 is a graphical representation of table III:1. The shortcoming of the solution in the form shown in figure III:2 is that the dimensionless parameters are referenced to the space-charge minimum and are not obviously related to experimentally observable quantities.

As discussed previously, the Maxwell-Boltzmann limit and the saturation current condition correspond to zero field at the collector (space-charge minimum at collector surface) and zero field (minimum) at emitter, respectively. The two zero-field conditions at the surfaces immediately relate the potential distribution in the interelectrode space to the applied voltage and are therefore the logical starting points for space-charge analysis.

A graphical representation of the space-charge relations is given in figure III:3. The form is similar to figure II:1; however, potential and distance are represented in dimensionless units. The relation between surface potential, work function, and Fermi level is as before, except the potential differences have been divided by kT/q to make them dimensionless. The potential distribution for zero field at the emitter is completely described by curve C-R (fig. III:3), which is the generalized solution of the space-charge conditions in the collector region. The location of the collector surface is established by the values of J , T , and w (i.e., the dimensionless distance x).

$$+\chi = \frac{1.442 \times 10^7 J^{1/2} x}{T^{3/4}} \text{ for singly charged cesium ions}$$

$$-\chi = \frac{6.5 \times 10^5 J^{1/2} x}{T^{3/4}} \text{ for electrons}$$

Emitter
temperature
 $^{\circ}\text{K}$ eV

.30
.28
3000 .26
2800 .24
2600 .22
2400 .20
2200 .18
2000 .16
1800 .14
1600 .12
1400 .10
1200 .08
1000 .06

Typical solution for
electrons; $T = 1800^{\circ}\text{K}$;
 $J = 3.0 \text{ amp}$; $x = 6 \mu$; and
 $\chi = 2.4$ (Specification of
any three terms is suf-
ficient.)

Current density
 $\mu\text{A/cm}^2$ A/cm^2

10 000
1 000
100
10
1
.1
.08
.06
.04
.02
1
.01
.008
.006
.004

L R

Dimensionless
distance,
 X

Cesium
ions
Electrons

400
200
100
80
60
40
20
10
8
6
4
2
1
.1
.01

A+ B-

Spacing, x
Cesium ions
 cm μ

.1 10
.8
6
4
2

L R L R

/ Indexing
line

Figure III:1. - Solutions of dimensionless distance parameter for singly charged cesium ions and electrons in ideal planar high vacuum diode. (Relations among current density, temperature, spacing, and zero field at collector surface are established for emitter of unlimited emission capability if nomographic solution is indexed at A or B (χ column) for ions and electrons, respectively.) Use only L or R columns for current density and spacing.

Conditions other than zero field at the emitter can be represented by the generalized space-charge curve (fig. III:2) displaced so that the potential curve corresponding to the emitter region passes through the point corresponding to the surface potential barrier at the surface of the emitter.

Several qualitative observations can be made with regard to figure III:3. Perhaps the most significant is the fact that the space-charge minimum must lie on a single curve (curve E-R) for all possible space-charge conditions. Curve E-R is the numerical solution of the space-charge relation (eq. III:4) in the emitter region and thus provides the means of analytically coupling the space-charge solution to the surface. Visualization of this relation is perhaps best achieved by using a procedure based on the simple graphical analysis of space-charge problems.

TABLE III:1. - NUMERICAL SOLUTION TO LANGMUIR EQUATION FOR SPACE CHARGE

(a) In emitter space (eq. (III:3))

Dimensionless potential, ψ_E	Dimensionless distance, X_E	$X_E^2, K^2 J x^2 / T^3 / 2$
a 0.50000 E-02	0.98671 E-01	0.97360 E-02
0.59999 E-02	0.10794 E-00	0.11652 E-01
0.70000 E-02	0.11645 E-00	0.13542 E-01
0.79999 E-02	0.12435 E-00	0.15464 E-01
0.89999 E-02	0.13176 E-00	0.17361 E-01
0.09999 E-01	0.13875 E-00	0.19251 E-01
0.11000 E-01	0.14538 E-00	0.21136 E-01
0.12000 E-01	0.15171 E-00	0.23016 E-01
0.13000 E-01	0.15776 E-00	0.24890 E-01
0.13999 E-01	0.16358 E-00	0.26760 E-01
0.15000 E-01	0.16919 E-00	0.28625 E-01
0.20000 E-01	0.19463 E-00	0.37883 E-01
0.24999 E-01	0.21689 E-00	0.47043 E-01
0.30000 E-01	0.23688 E-00	0.56114 E-01
0.34999 E-01	0.25515 E-00	0.65105 E-01
0.40000 E-01	0.27206 E-00	0.74201 E-01
0.45000 E-01	0.28786 E-00	0.82868 E-01
0.49999 E-01	0.30273 E-00	0.91649 E-01
0.59999 E-01	0.33019 E-00	0.10903 E-00
0.69999 E-01	0.35522 E-00	0.12618 E-00
0.80000 E-01	0.37832 E-00	0.14313 E-00
0.90000 E-01	0.39985 E-00	0.15988 E-00
0.09999 E-00	0.42005 E-00	0.17644 E-00
0.15000 E-00	0.50679 E-00	0.25684 E-00
0.20000 E-00	0.57767 E-00	0.33370 E-00
0.25000 E-00	0.63839 E-00	0.40754 E-00
0.30000 E-00	0.69188 E-00	0.47871 E-00
0.34999 E-00	0.73990 E-00	0.54745 E-00
0.40000 E-00	0.78356 E-00	0.61396 E-00
0.45000 E-00	0.82346 E-00	0.67882 E-00
0.49999 E-00	0.86078 E-00	0.74094 E-00
0.55000 E-00	0.89535 E-00	0.80165 E-00
0.59999 E-00	0.92770 E-00	0.86064 E-00
0.64999 E-00	0.95812 E-00	0.91800 E-00
0.70000 E-00	0.98681 E-00	0.97380 E-00
0.74999 E-00	0.10139 E-01	0.10281 E-01
0.79999 E-00	0.10397 E-01	0.10810 E-01
0.84999 E-00	0.10642 E-01	0.11325 E-01
0.89999 E-00	0.10875 E-01	0.11827 E-01
0.95000 E-00	0.11098 E-01	0.12316 E-01
0.99999 E-00	0.11311 E-01	0.12794 E-01
b 0.10500 E-01	0.11515 E-01	0.13259 E-01
0.10999 E-01	0.11710 E-01	0.13713 E-01
0.11499 E-01	0.11898 E-01	0.14156 E-01
0.11999 E-01	0.12078 E-01	0.14588 E-01
0.12499 E-01	0.12251 E-01	0.15010 E-01
0.13000 E-01	0.12418 E-01	0.15422 E-01
0.13499 E-01	0.12579 E-01	0.15824 E-01
0.13999 E-01	0.12734 E-01	0.16216 E-01
0.14500 E-01	0.12884 E-01	0.16599 E-01
0.14999 E-01	0.13028 E-01	0.16973 E-01
0.16000 E-01	0.13302 E-01	0.17696 E-01
0.16999 E-01	0.13559 E-01	0.18385 E-01
0.17999 E-01	0.13799 E-01	0.19042 E-01
0.19000 E-01	0.14024 E-01	0.19669 E-01
0.20000 E-01	0.14236 E-01	0.20268 E-01
0.20999 E-01	0.14436 E-01	0.20804 E-01
0.21999 E-01	0.14623 E-01	0.21386 E-01
0.23000 E-01	0.14800 E-01	0.21906 E-01
0.23999 E-01	0.14968 E-01	0.22404 E-01
0.24999 E-01	0.15125 E-01	0.22878 E-01
0.25999 E-01	0.15274 E-01	0.23332 E-01
0.27000 E-01	0.15415 E-01	0.23764 E-01
0.27999 E-01	0.15549 E-01	0.24177 E-01
0.28999 E-01	0.15675 E-01	0.24571 E-01
0.29999 E-01	0.15795 E-01	0.24948 E-01
0.30999 E-01	0.15908 E-01	0.25307 E-01
0.31999 E-01	0.16015 E-01	0.25650 E-01
0.32999 E-01	0.16117 E-01	0.25977 E-01
0.34000 E-01	0.16213 E-01	0.26289 E-01
0.34999 E-01	0.16305 E-01	0.26587 E-01
0.35999 E-01	0.16392 E-01	0.26871 E-01
0.38000 E-01	0.16553 E-01	0.27400 E-01
0.40000 E-01	0.16698 E-01	0.27882 E-01
0.41999 E-01	0.16828 E-01	0.28321 E-01
0.43999 E-01	0.16946 E-01	0.28719 E-01
0.45999 E-01	0.17053 E-01	0.29081 E-01
0.47999 E-01	0.17149 E-01	0.29410 E-01
0.49999 E-01	0.17236 E-01	0.29709 E-01
0.55000 E-01	0.17419 E-01	0.30342 E-01
0.59995 E-01	0.17560 E-01	0.30838 E-01
0.64999 E-01	0.17671 E-01	0.31227 E-01
0.70000 E-01	0.17757 E-01	0.31531 E-01
0.74999 E-01	0.17823 E-01	0.31769 E-01
0.80000 E-01	0.17876 E-01	0.31955 E-01
0.89999 E-01	0.17948 E-01	0.32213 E-01
0.11000 E-02	0.17991 E-01	0.32370 E-01
0.12000 E-02	0.18034 E-01	0.32523 E-01
0.13000 E-02	0.18052 E-01	0.32580 E-01
0.16000 E-02	0.18055 E-01	0.32601 E-01
0.18000 E-02	0.18057 E-01	0.32608 E-01
0.20000 E-02	0.18058 E-01	0.32611 E-01

(b) In collector space (eq. (III:3))

Dimensionless potential, ψ_C	Dimensionless distance, X_C	$X_C^2, K^2 J x^2 / T^3 / 2$
c 0.09999 E-01	0.14406 E-00	0.20756 E-01
0.20000 E-01	0.20527 E-00	0.42138 E-01
0.30000 E-01	0.25284 E-00	0.63929 E-01
0.40000 E-01	0.29334 E-00	0.86052 E-01
0.49999 E-01	0.32933 E-00	0.10846 E-00
0.59999 E-01	0.36211 E-00	0.13112 E-00
0.69999 E-01	0.39246 E-00	0.15402 E-00
0.79999 E-01	0.42088 E-00	0.17714 E-00
0.89999 E-01	0.44773 E-00	0.20046 E-00
0.99999 E-01	0.47325 E-00	0.22397 E-00
0.15000 E-00	0.58660 E-00	0.34410 E-00
0.20000 E-00	0.68409 E-00	0.46798 E-00
0.25000 E-00	0.77114 E-00	0.59509 E-00
0.30000 E-00	0.85153 E-00	0.72511 E-00
0.34999 E-00	0.92616 E-00	0.85777 E-00
0.40000 E-00	0.99644 E-00	0.99289 E-00
0.45000 E-00	0.10631 E-01	0.11303 E-01
0.49999 E-00	0.11268 E-01	0.12699 E-01
0.60000 E-00	0.12470 E-01	0.15551 E-01
0.70000 E-00	0.13593 E-01	0.18479 E-01
0.80000 E-00	0.14655 E-01	0.21477 E-01
d 0.90000 E-00	0.15665 E-01	0.24540 E-01
0.99999 E-01	0.16632 E-01	0.27665 E-01
0.10999 E-01	0.17563 E-01	0.30849 E-01
0.12000 E-01	0.18463 E-01	0.34088 E-01
0.13000 E-01	0.20180 E-01	0.40726 E-01
0.14000 E-01	0.23363 E-01	0.47562 E-01
0.15000 E-01	0.24856 E-01	0.54584 E-01
0.16000 E-01	0.26295 E-01	0.61782 E-01
0.17000 E-01	0.27689 E-01	0.69146 E-01
0.18000 E-01	0.29042 E-01	0.76669 E-01
0.19000 E-01	0.30399 E-01	0.84345 E-01
0.20000 E-01	0.32799 E-01	0.92167 E-01
0.21000 E-01	0.34203 E-01	0.10012 E-02
0.22000 E-01	0.35829 E-01	0.10822 E-02
0.23000 E-01	0.34126 E-01	0.11646 E-02
0.24000 E-01	0.35329 E-01	0.12481 E-02
0.25000 E-01	0.36510 E-01	0.13330 E-02
0.26000 E-01	0.37670 E-01	0.14190 E-02
0.27000 E-01	0.38768 E-01	0.14939 E-02
0.28000 E-01	0.40488 E-01	0.16393 E-02
0.29000 E-01	0.43203 E-01	0.18665 E-02
0.30000 E-01	0.45829 E-01	0.21003 E-02
0.31000 E-01	0.48378 E-01	0.23404 E-02
0.32000 E-01	0.50859 E-01	0.25866 E-02
0.33000 E-01	0.53279 E-01	0.28386 E-02
0.34000 E-01	0.55663 E-01	0.30962 E-02
0.35000 E-01	0.57598 E-01	0.33592 E-02
0.36000 E-01	0.62455 E-01	0.39007 E-02
0.37000 E-01	0.66798 E-01	0.44620 E-02
0.38000 E-01	0.71007 E-01	0.50420 E-02
0.39000 E-01	0.75099 E-01	0.56399 E-02
0.40000 E-01	0.79087 E-01	0.62548 E-02
0.41000 E-01	0.82982 E-01	0.68860 E-02
0.42000 E-01	0.86790 E-01	0.75326 E-02
0.43000 E-01	0.90515 E-01	0.81930 E-02
0.44000 E-01	0.97683 E-01	0.95420 E-02
0.45000 E-01	0.10378 E-01	0.10772 E-03
0.46000 E-01	0.12052 E-01	0.14526 E-03
0.47000 E-01	0.13630 E-01	0.18580 E-03
0.48000 E-01	0.15134 E-02	0.22906 E-03
0.49000 E-01	0.16578 E-02	0.27484 E-03
0.50000 E-01	0.17971 E-02	0.32298 E-03
0.51000 E-01	0.19322 E-02	0.37334 E-03
0.52000 E-01	0.21915 E-02	0.48027 E-03
0.53000 E-01	0.24390 E-02	0.59488 E-03
0.54000 E-01	0.26769 E-02	0.71661 E-03
0.55000 E-01	0.29048 E-02	0.84498 E-03
0.56000 E-01	0.31298 E-02	0.97961 E-03
0.57000 E-01	0.34167 E-02	0.17367 E-04
0.58000 E-01	0.41674 E-02	0.26158 E-04
0.59000 E-01	0.51145 E-02	0.46781 E-04
0.60000 E-01	0.68397 E-02	0.70848 E-04
0.61000 E-01	0.84171 E-02	0.109291 E-03
0.62000 E-01	0.11295 E-02	0.15181 E-03
0.63000 E-01	0.16398 E-02	0.23048 E-05

^aRead as 0.5×10^{-2} .^bRead as 0.105×10^1 .^cRead as 0.09×10^{-1} .^dRead as 0.09×10^1 .

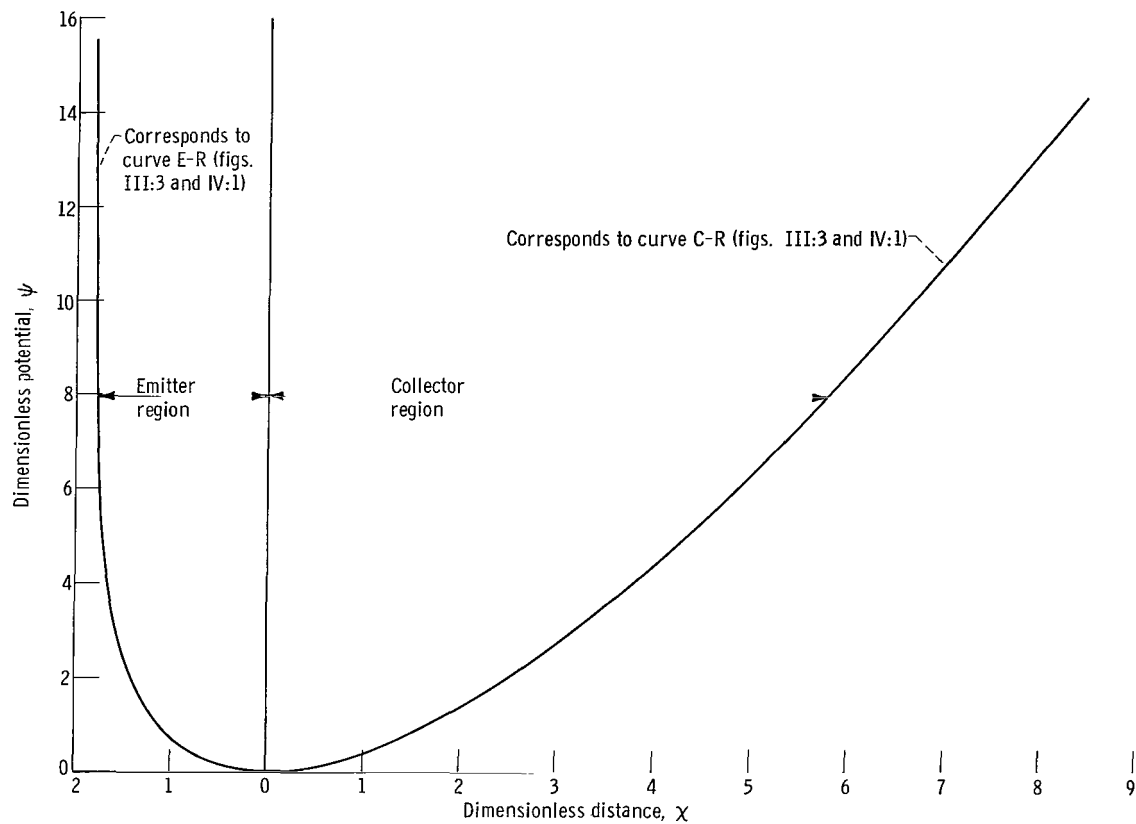


Figure III:2. - Space-charge potential distribution.

A "template" can be made to represent the generalized space-charge solution corresponding to the form given in figure III:2. Starting with zero field at the emitter the space-charge minimum of the template must coincide with the potential at the surface barrier, for example, point 1 in figure III:3. The potential distribution in the interelectrode space can then be drawn and must lie on curve C-R. By noting that the generalized space-charge curve must always cross the surface at point 1, the "space-charge template" then may be shifted to correspond to ever increasing space-charge barriers. (Coordinates must of course be maintained parallel). The magnitude and location of the barrier are described by the position of the minimum. (The reader should note that dimensionless distance X contains $J^{1/2}$, which decreases as the space-charge barrier becomes larger, therefore distorting the real distance feature of the potential curve.) Examples of the location of the minimum and corresponding potential distributions have been constructed by this procedure and are illustrated in figure III:3 (pt. 2' curve II, pt. 3' curve III, etc.). In the process of shifting the space-charge template from the zero-field condition to curve XIII (for example), the space-charge minimum will trace out curve E-R, which as indicated before is the emitter region branch of the generalized space-charge curve. From the nature of the emitter region space-charge solution, the location of the space-charge minimum cannot exceed a value of $X = 1.806$: Thus not only is the location of the minimum completely described but also the limits of $X_E = 0$ and 1.806. Curve E-R also represents all possible locations of the

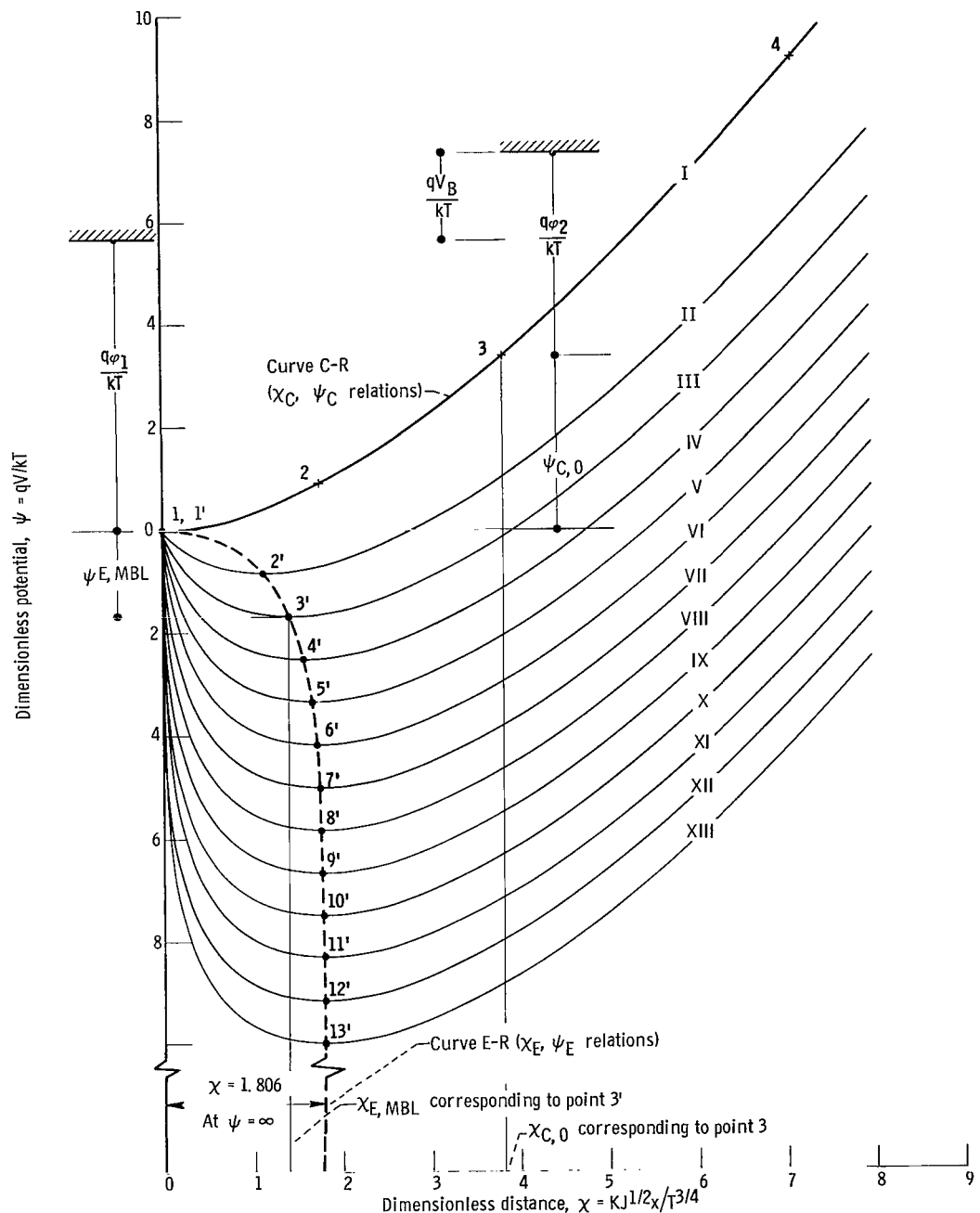


Figure III:3. - Generalized space-charge potential distributions.

collector surface in terms of dimensionless distance at the Maxwell-Boltzmann limit, since by definition zero field at the collector must exist at this limiting condition.

If distance, saturation current, and temperature are held constant ($x_{C,0}$ = constant) while applied voltage is varied, then it is possible to uniquely establish the current at the Maxwell-Boltzmann limit and thus $x_{E,MBL}$. The related quantities $\psi_{E,MBL}$ and difference in surface potential between saturation current and the current at the MBL condition ($\psi_{C,0} + \psi_{E,MBL}$) follow directly. The general procedure employed is perhaps best illustrated by example. Let the saturation current, distance, and temperature correspond to a value of $x_{C,0}$ represented by point 3 on curve C-R figure III:3. At the Maxwell-Boltzmann condition (i.e., zero-field condition at the collector) the current will be inhibited by the space-charge barrier, which is identifiable since the barrier is at the collector surface. The barrier height is $\psi_{E,MBL}$, and the reduction in current is determined from the Boltzmann relation

$$\frac{J_{MBL}}{J_0} = \exp(-\psi_{E,MBL}) \quad (III:5)$$

Numerical or graphical iteration quickly determines the value of x_E (point 3' must lie on the x_E curve) that satisfies equation (III:5) and the x_E, ψ_E space-charge relation. Point 3' is thus uniquely established. In a similar sense point 2 corresponds to point 2' or for larger values of $x_{C,0}$ point 4 corresponds to point 4', 5 to 5', and so forth.

Further detailed developments of the relation between the two zero-field conditions and the parametric relations involving current, distance, temperature, and mass to charge ratio are given in section IV.

It again should be noted that the key to the numerical solution of the space-charge problem is based on the two zero-field conditions, when the space-charge barrier exists at the emitter and at the collector. Also it is interesting to note that as $\psi_{E,MBL}$ approaches infinity, $x_{E,MBL}$ possesses a limiting value of 1.806. For all practical purposes when $\psi_{E,MBL}$ is greater than 10, $x_{E,MBL}$ has approached the limiting value. Use will be made of this fact in section VII in the development of a universal unlimited current-voltage curve.

IV - ANALYTICAL DEVELOPMENT OF SPACE-CHARGE RELATIONS

Assume that in a hypothetical case, the emitter temperature, spacing, and current at the Maxwell-Boltzmann limit are known and the objective is to determine the saturation current. The dimensionless distance $x_{E,MBL}$ is now defined since

$$x_{E,MBL} = \frac{\frac{KJ^{1/2}}{MBL^W}}{T^{3/4}} \quad (IV:1)$$

The dimensionless potential $\psi_{E,MBL}$ is also established from the generalized

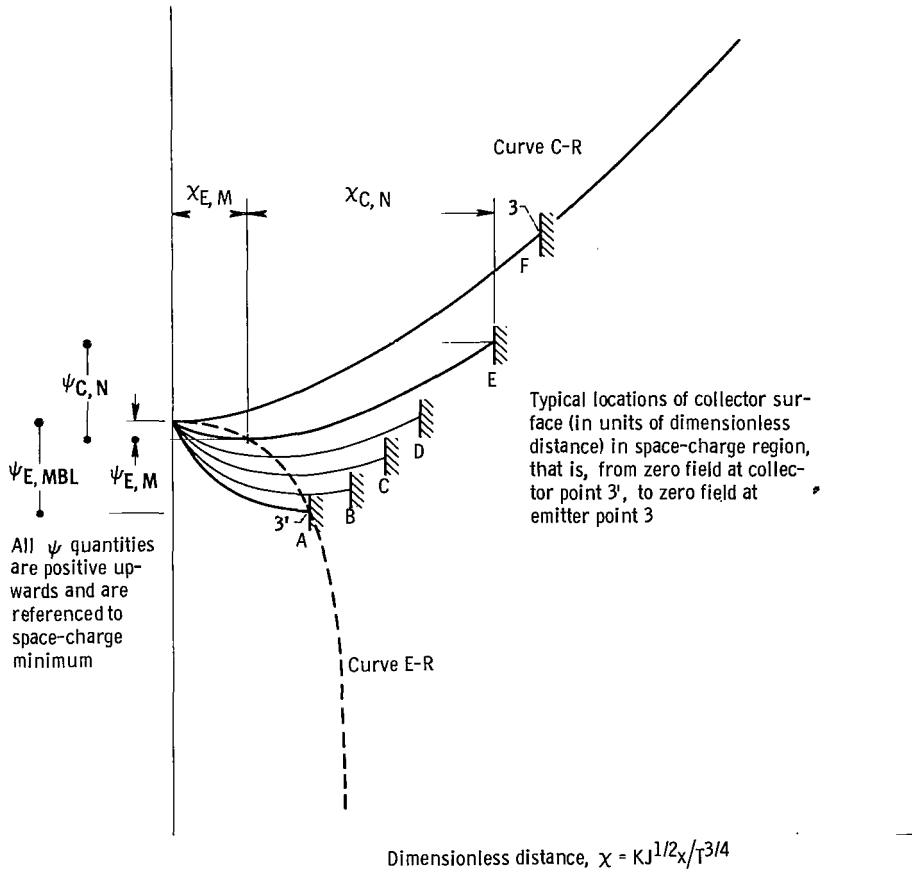


Figure IV:1. - Typical transition potential diagrams in space-charge region.

space-charge relation (table III:1(a) for example). As the applied voltage is made more positive (for electrons), the potential distribution varies as shown in figure IV:1. The collector location in units of X shifts to the right because of the increase in current. The space-charge barrier shifts from the collector surface (curve A) into the interelectrode space (curves B, C, D, and E) and finally intercepts the emitter surface (curve F). The structure of figure IV:1 is identical to that of figure III:3 (p. 10) except for the increased detail for the transition conditions between points $3'$ and 3 .

As indicated in section III, current will increase up to J_0 between the Maxwell-Boltzmann limit and the saturation condition according to the following relations:

$$J_0 = J_{MBL} \exp(\phi_{E,MBL}) = J_{MBL} f(X_{MBL}) \quad (IV:2)$$

where J_0 is now the saturation current since zero field exists at the emitter. The numerical evaluation of the ratio of J_0/J_{MBL} for various values of $X_{E,MBL}$ is given in figure IV:2. The combination of figure IV:2 and the nomograph in figure III:1 (p. 7) conveniently relates saturation current to J_{MBL} ,

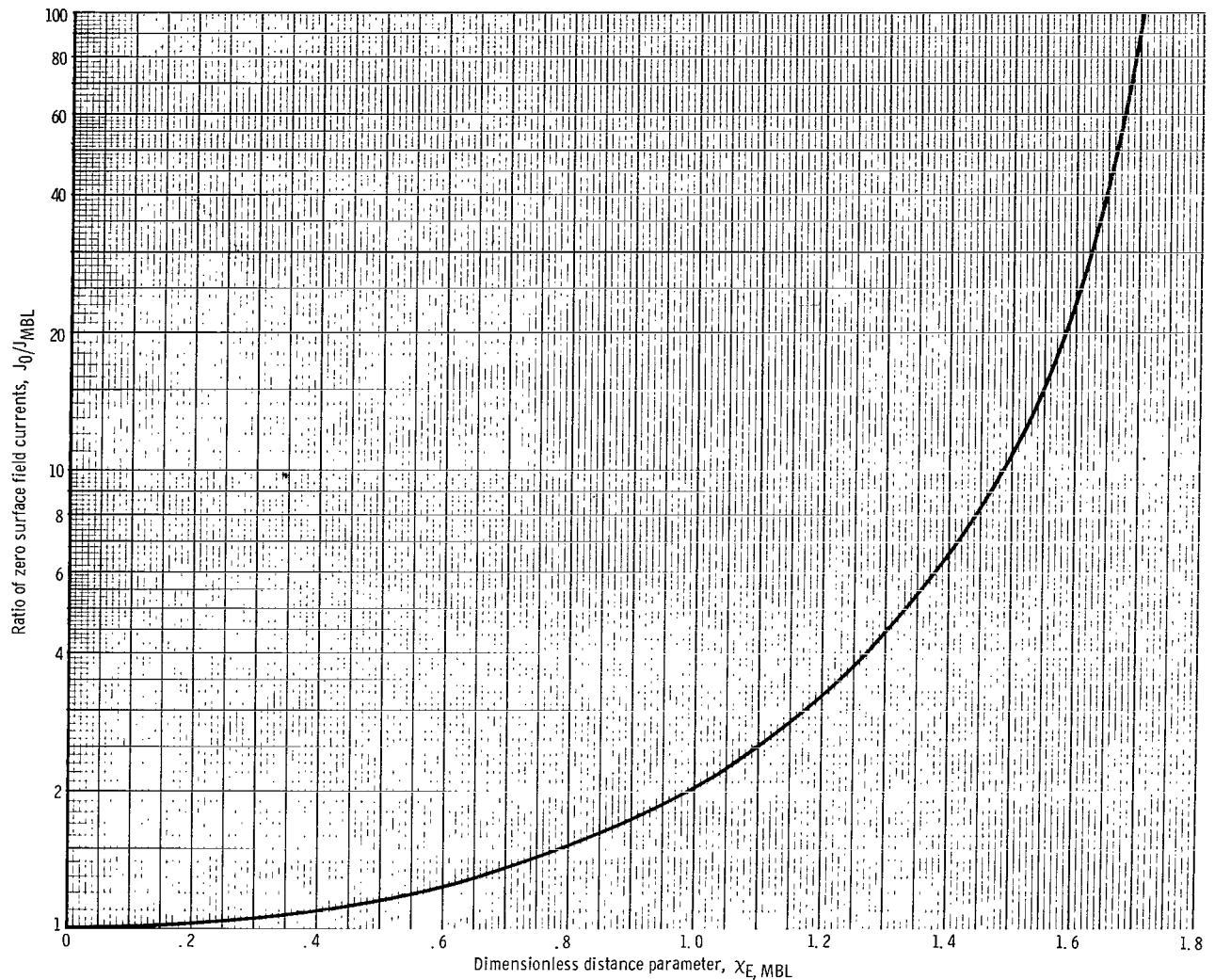


Figure IV:2. - Relation between dimensionless distance evaluated at condition of zero field at collector and ratio of current densities J_0/J_{MBL} .

spacing, and emitter temperature. $X_{E,MBL}$ is determined from the nomograph (fig. III:1) for either ions or electrons, and J_0 is subsequently established from figure IV:2.

Additional useful relations can also be determined from an extension of the approach used previously. Since the saturation current is known, the dimensionless distance in the collector region is

$$X_{C,0} = X_{E,MBL} \exp\left(\frac{\psi_{E,MBL}}{2}\right) \quad (IV:3)$$

(All terms in X are constant except current.) The dimensionless potential $\psi_{C,0}$ is established from $X_{C,0}$ (the subscript 0 again refers to zero field at the emitter surface), and therefore the variation in surface potential in

TABLE IV:1. - TABULATIONS OF VARIATION IN APPLIED VOLTAGE (DIFFERENCE IN SURFACE POTENTIAL) THAT EXISTS BETWEEN MAXWELL-BOLTZMANN LIMIT AND SATURATED CURRENT CONDITION FOR IDEAL PLANAR HIGH VACUUM DIODE

[Temperature, distance, and saturation current capability are assumed constant.]

(a) Tabulation for even values of surface potential

Surface potential difference, $\psi_{E,MEL} + \psi_{C,0}$	Dimensionless distance corresponding to -	Current ratio, J_0/J_{MEL}
	Zero field at emitter, $X_{C,0}$	Zero field at collector, $X_{E,MEL}$
0.09999 E-01	0.10007 E-00	0.99822 E-01
0.20000 E-01	0.14165 E-00	0.14092 E-00
a.30000 E-01	0.17365 E-00	0.17231 E-00
0.40000 E-01	0.20071 E-00	0.19862 E-00
0.49999 E-01	0.22461 E-00	0.22170 E-00
0.59999 E-01	0.24630 E-00	0.24245 E-00
0.69999 E-01	0.26630 E-00	0.26144 E-00
0.79999 E-01	0.28497 E-00	0.27903 E-00
0.90000 E-01	0.30257 E-00	0.29547 E-00
0.09999 E-00	0.31927 E-00	0.31094 E-00
0.15000 E-00	0.39315 E-00	0.37778 E-00
0.20000 E-00	0.45652 E-00	0.43281 E-00
0.25000 E-00	0.51329 E-00	0.48017 E-00
0.30000 E-00	0.56548 E-00	0.52200 E-00
0.34999 E-00	0.61429 E-00	0.55961 E-00
0.40000 E-00	0.66051 E-00	0.59388 E-00
0.45000 E-00	0.70457 E-00	0.62531 E-00
0.49999 E-00	0.74695 E-00	0.65443 E-00
0.60000 E-00	0.82767 E-00	0.70698 E-00
0.70000 E-00	0.90420 E-00	0.75337 E-00
0.80000 E-00	0.97751 E-00	0.79485 E-00
0.90000 E-00	0.10482 E-01	0.83232 E-00
0.09999 E-01	0.11169 E-01	0.86642 E-00
0.10999 E-01	0.11838 E-01	0.89767 E-00
0.12000 E-01	0.12493 E-01	0.92645 E-00
0.13999 E-01	0.13766 E-01	0.97784 E-00
0.16000 E-01	0.14999 E-01	0.10225 E-01
0.17999 E-01	0.16201 E-01	0.10618 E-01
0.20000 E-01	0.17375 E-01	0.10967 E-01
0.21999 E-01	0.18527 E-01	0.11279 E-01
0.23999 E-01	0.19659 E-01	0.11561 E-01
0.26000 E-01	0.20772 E-01	0.11916 E-01
0.27999 E-01	0.21869 E-01	0.12049 E-01
0.30000 E-01	0.22951 E-01	0.12263 E-01
0.31999 E-01	0.24019 E-01	0.12459 E-01
0.34000 E-01	0.25074 E-01	0.12640 E-01
0.35999 E-01	0.26117 E-01	0.12809 E-01
0.38000 E-01	0.27148 E-01	0.12965 E-01
0.39999 E-01	0.28167 E-01	0.13110 E-01
0.45000 E-01	0.30673 E-01	0.13435 E-01
0.49999 E-01	0.33120 E-01	0.13713 E-01
0.55000 E-01	0.35515 E-01	0.13954 E-01
0.59999 E-01	0.37862 E-01	0.14166 E-01
0.64999 E-01	0.40164 E-01	0.14353 E-01
0.70000 E-01	0.42426 E-01	0.14520 E-01
0.74999 E-01	0.44650 E-01	0.14671 E-01
0.80000 E-01	0.46840 E-01	0.14806 E-01
0.89999 E-01	0.51118 E-01	0.15042 E-01
0.09999 E-02	0.55282 E-01	0.15241 E-01
0.11000 E-02	0.59341 E-01	0.15411 E-01
0.12000 E-02	0.63305 E-01	0.15558 E-01
0.13000 E-02	0.67188 E-01	0.15687 E-01
b.13999 E-02	0.70984 E-01	0.15800 E-01
0.15000 E-02	0.74713 E-01	0.15902 E-01
0.16000 E-02	0.78377 E-01	0.15993 E-01
0.18000 E-02	0.85529 E-01	0.16150 E-01
0.20000 E-02	0.92470 E-01	0.16281 E-01
0.25000 E-02	0.10904 E-02	0.16532 E-01
0.30000 E-02	0.12472 E-02	0.16711 E-01
0.34999 E-02	0.13970 E-02	0.16847 E-01
0.40000 E-02	0.15411 E-02	0.16954 E-01
0.45000 E-02	0.16802 E-02	0.17041 E-01
0.50000 E-02	0.18149 E-02	0.17113 E-01
0.59999 E-02	0.20743 E-02	0.17226 E-01
0.70000 E-02	0.23145 E-02	0.17309 E-01
0.80000 E-02	0.25549 E-02	0.17377 E-01
0.90000 E-02	0.27872 E-02	0.17432 E-01
0.09999 E-03	0.30041 E-02	0.17476 E-01
0.15000 E-03	0.40406 E-02	0.17622 E-01
0.20000 E-03	0.49864 E-02	0.17703 E-01
0.30000 E-03	0.67092 E-02	0.17793 E-01
0.40000 E-03	0.82721 E-02	0.17843 E-01
0.50000 E-03	0.97836 E-02	0.17876 E-01
0.60000 E-03	0.10991 E-03	0.17895 E-01
0.70000 E-03	0.12262 E-03	0.17912 E-01
0.80000 E-03	0.13583 E-03	0.17926 E-01
0.90000 E-03	0.14942 E-03	0.17938 E-01
0.09999 E-04	0.16321 E-03	0.17948 E-01

^aRead as 0.3×10^{-1} .

^bRead as 0.15×10^2 .

TABLE IV:1. - Continu-1. TABULATIONS OF VARIATION IN APPLIED VOLTAGE
(DIPPERHOLZ IN SURFACE POTENTIAL) THAT EXISTS BETWEEN MAXWELL-BOLTZMANN LIMIT AND SATURATED CURRENT CONDITION FOR IDEAL PLANAR HIGH VACUUM DIODE

[Temperature, distance, and saturation current capability are assumed constant.]

(b) Tabulator for even values of $X_{E,MEL}$ (dimensionless distance at zero field at collector)

Surface potential difference, $E_{E,MEL} + \psi_{C,0}$	Dimensionless distance corresponding to -		Current ratio, J_0/J_{MEL}
	Zero field at emitter, $X_{E,0}$	Zero field at collector, $X_{E,MEL}$	
0.10034 E-01	0.10025 E-00	0.09999 E-00	0.10051 E 01
0.12030 E-01	0.12034 E-00	0.11000 E-00	0.10062 E 01
0.14034 E-01	0.12040 E-00	0.12000 E-00	0.10073 E 01
0.16038 E-01	0.12057 E-00	0.13000 E-00	0.10084 E 01
0.18035 E-01	0.12063 E-00	0.13500 E-00	0.10095 E 01
0.19733 E-01	0.12071 E-00	0.13999 E-00	0.10102 E 01
0.21178 E-01	0.12079 E-00	0.14500 E-00	0.10110 E 01
0.22267 E-01	0.12086 E-00	0.15000 E-00	0.10117 E 01
0.23262 E-01	0.12093 E-00	0.15500 E-00	0.10123 E 01
0.27482 E-01	0.12107 E-00	0.16500 E-00	0.10133 E 01
0.29191 E-01	0.12129 E-00	0.16999 E-00	0.10152 E 01
0.30956 E-01	0.12164 E-00	0.17500 E-00	0.10162 E 01
0.32772 E-01	0.12183 E-00	0.18000 E-00	0.10171 E 01
0.34640 E-01	0.12187 E-00	0.18499 E-00	0.10181 E 01
0.36518 E-01	0.12191 E-00	0.18999 E-00	0.10192 E 01
0.38523 E-01	0.12196 E-00	0.19499 E-00	0.10202 E 01
0.40551 E-01	0.12202 E-00	0.20600 E-00	0.10213 E 01
0.44777 E-01	0.12212 E-00	0.20999 E-00	0.10236 E 01
0.53879 E-01	0.12332 E-00	0.23000 E-00	0.10286 E 01
0.63871 E-01	0.12542 E-00	0.25000 E-00	0.10341 E 01
0.73873 E-01	0.12753 E-00	0.27000 E-00	0.10400 E 01
0.84508 E-01	0.12870 E-00	0.29000 E-00	0.10447 E 01
0.92648 E-01	0.12974 E-00	0.30000 E-00	0.10502 E 01
0.11311 E-00	0.13400 E-00	0.33000 E-00	0.10617 E 01
0.12783 E-00	0.13620 E-00	0.34999 E-00	0.10701 E 01
0.14358 E-00	0.13843 E-00	0.37000 E-00	0.10792 E 01
0.16000 E-00	0.14044 E-00	0.39000 E-00	0.10890 E 01
0.16915 E-00	0.14182 E-00	0.40000 E-00	0.10923 E 01
0.18760 E-00	0.14192 E-00	0.41193 E-00	0.11051 E 01
0.22776 E-00	0.148879 E-00	0.45999 E-00	0.11291 E 01
0.24972 E-00	0.151305 E-00	0.48000 E-00	0.11424 E 01
0.27297 E-00	0.153776 E-00	0.50000 E-00	0.11424 E 01
0.33303 E-00	0.160162 E-00	0.53000 E-00	0.11567 E 01
0.35933 E-00	0.16144 E-00	0.55000 E-00	0.11615 E 01
0.459770 E-00	0.17126 E-00	0.63000 E-00	0.12430 E 01
0.56611 E-00	0.18002 E-00	0.69000 E-00	0.12746 E 01
0.58576 E-00	0.181656 E-00	0.70000 E-00	0.13473 E 01
0.64802 E-00	0.186495 E-00	0.73000 E-00	0.13607 E 01
0.76290 E-00	0.195067 E-00	0.79000 E-00	0.14039 E 01
0.81400 E-00	0.200000 E-00	0.80000 E-00	0.14250 E 01
0.86598 E-00	0.10244 E-01	0.81199 E-00	0.15218 E 01
0.90845 E-00	0.11036 E-01	0.86000 E-00	0.15608 E 01
0.10425 E-01	0.11455 E-01	0.88000 E-00	0.16469 E 01
0.11177 E-01	0.11889 E-01	0.90000 E-00	0.16946 E 01
0.11768 E-01	0.12343 E-01	0.91999 E-00	0.17452 E 01
0.12769 E-01	0.12656 E-01	0.93999 E-00	0.18049 E 01
0.13271 E-01	0.12837 E-01	0.95999 E-00	0.18895 E 01
0.14590 E-01	0.13822 E-01	0.98000 E-00	0.19216 E 01
0.14956 E-01	0.14361 E-01	0.09999 E 01	0.19895 E 01
0.15411 E-01	0.14640 E-01	0.10100 E 01	0.20223 E 01
0.16361 E-01	0.15219 E-01	0.10249 E 01	0.21012 E 01
0.17101 E-01	0.15526 E-01	0.10400 E 01	0.21525 E 01
0.17500 E-01	0.15642 E-01	0.10599 E 01	0.22720 E 01
0.19121 E-01	0.16799 E-01	0.10800 E 01	0.23192 E 01
0.20196 E-01	0.17491 E-01	0.10999 E 01	0.24195 E 01
0.20822 E-01	0.17852 E-01	0.11199 E 01	0.25283 E 01
0.22135 E-01	0.18605 E-01	0.11300 E 01	0.25867 E 01
0.23543 E-01	0.19403 E-01	0.11400 E 01	0.26101 E 01
0.25557 E-01	0.20251 E-01	0.11997 E 01	0.28469 E 01
0.27554 E-01	0.21255 E-01	0.11900 E 01	0.29959 E 01
0.29393 E-01	0.22620 E-01	0.12199 E 01	0.31598 E 01
0.31368 E-01	0.23685 E-01	0.12400 E 01	0.32475 E 01
0.32425 E-01	0.24246 E-01	0.12499 E 01	0.34379 E 01
0.34778 E-01	0.259430 E-01	0.12700 E 01	0.37624 E 01
0.36152 E-01	0.26057 E-01	0.12899 E 01	0.40097 E 01
0.38485 E-01	0.26193 E-01	0.13000 E 01	0.41442 E 01
0.42207 E-01	0.29586 E-01	0.13239 E 01	0.44365 E 01
0.44688 E-01	0.31213 E-01	0.13500 E 01	0.49479 E 01
0.49731 E-01	0.32993 E-01	0.13639 E 01	0.57997 E 01
0.55599 E-01	0.35990 E-01	0.13999 E 01	0.66088 E 01
0.60155 E-01	0.36274 E-01	0.14000 E 01	0.72582 E 01
0.66372 E-01	0.40468 E-01	0.14399 E 01	0.80154 E 01
0.69338 E-01	0.42131 E-01	0.14500 E 01	0.84425 E 01
0.72566 E-01	0.43574 E-01	0.14600 E 01	0.89074 E 01
0.79742 E-01	0.46727 E-01	0.14799 E 01	0.92462 E 01
0.86041 E-01	0.50290 E-01	0.15000 E 01	0.11240 E 02
0.92723 E-01	0.52243 E-01	0.15297 E 01	0.11979 E 02
0.98500 E-01	0.55613 E-01	0.15300 E 01	0.12794 E 02
1.03299 E-01	0.56461 E-01	0.15300 E 01	0.13700 E 02
1.09311 E-01	0.59063 E-01	0.15399 E 01	0.14109 E 02
1.11599 E-01	0.61686 E-01	0.15499 E 01	0.15068 E 02
0.12312 E-01	0.64524 E-01	0.15600 E 01	0.17108 E 02
0.13110 E-01	0.67666 E-01	0.15700 E 01	0.18542 E 02
0.14082 E-01	0.70708 E-01	0.15799 E 01	0.20172 E 02
0.14678 E-01	0.74632 E-01	0.15839 E 01	0.22032 E 02
0.16072 E-01	0.78643 E-01	0.16000 E 01	0.24159 E 02
0.17313 E-01	0.83100 E-01	0.16100 E 01	0.27494 E 02
0.18711 E-01	0.88023 E-01	0.16199 E 01	0.29523 E 02
0.20203 E-01	0.93508 E-01	0.16300 E 01	0.32909 E 02
0.22438 E-01	0.10658 E-02	0.16400 E 01	0.36924 E 02
0.26702 E-01	0.11448 E-02	0.16599 E 01	0.41331 E 02
0.29616 E-01	0.12156 E-02	0.16700 E 01	0.54745 E 02
0.33086 E-01	0.13466 E-02	0.16800 E 01	0.63681 E 02
0.37300 E-01	0.14641 E-02	0.16899 E 01	0.75058 E 02
0.42482 E-01	0.15700 E-02	0.16999 E 01	0.89699 E 02
0.48566 E-01	0.17811 E-02	0.17100 E 01	0.10930 E 03
0.57308 E-01	0.20061 E-02	0.17200 E 01	0.11900 E 03
0.68179 E-01	0.22780 E-02	0.17299 E 01	0.17340 E 03
0.83487 E-01	0.26418 E-02	0.17399 E 01	0.23051 E 03
0.10512 E-01	0.31263 E-02	0.17500 E 01	0.31916 E 03
0.13536 E-01	0.37491 E-02	0.17699 E 01	0.47288 E 03
0.19547 E-01	0.49104 E-02	0.17693 E 01	0.77249 E 03
0.30768 E-01	0.68566 E-02	0.17800 E 01	0.11791 E 07
0.60563 E-01	0.11269 E-03	0.17900 E 01	0.39636 E 04
0.19450 E-04	0.26639 E-03	0.17999 E 01	0.21903 E 05
0.28478 E-05	0.19599 E-04	0.18049 E 01	0.11791 E 07

^a Read as 0.10034×10^{-1} .

^b Read as 0.19547×10^3 .

TABLE IV:1. - Concluded. TABULATIONS OF VARIATION IN APPLIED VOLTAGE
(DIFFERENCE IN SURFACE POTENTIAL) THAT EXISTS BETWEEN MAXWELL-
BOLTZMANN LIMIT AND SATURATED CURRENT CONDITION FOR
IDEAL PLANAR HIGH VACUUM DIODE
[Temperature, distance, and saturation current capability are assumed
constant.]
(c) Tabulation for even values of $x_{C,0}$ (dimensionless distance
at zero field at emitter)

Surface potential difference, $x_{B,MHL} + x_{C,0}$	Dimensionless distance corresponding to " "	Zero field at emitter, $x_{C,0}$	Zero field at collector, $x_{E,MHL}$	Current ratio, J_0/J_{MHL}
a 0.22407 E-01	0.15000 E-00	0.14909 E-00	0.10121 E 01	
0.39111 E-01	0.20000 E-00	0.19790 E-00	0.10212 E 01	
0.47707 E-01	0.25000 E-00	0.24597 E-00	0.10330 E 01	
0.88477 E-01	0.30000 E-00	0.29400 E-00	0.10482 E 01	
0.100644 E-00	0.31999 E-00	0.31160 E-00	0.10545 E 01	
0.11308 E-00	0.34000 E-00	0.32935 E-00	0.10617 E 01	
0.11966 E-00	0.34999 E-00	0.33906 E-00	0.10655 E 01	
0.12641 E-00	0.36000 E-00	0.34812 E-00	0.10694 E 01	
0.14442 E-00	0.38000 E-00	0.36608 E-00	0.10774 E 01	
0.15558 E-00	0.40000 E-00	0.38491 E-00	0.10799 E 01	
0.17039 E-00	0.41999 E-00	0.40133 E-00	0.10951 E 01	
0.18452 E-00	0.43999 E-00	0.41867 E-00	0.11104 E 01	
0.19456 E-00	0.45000 E-00	0.43600 E-00	0.11293 E 01	
C 20292 E-00	0.45999 E-00	0.43574 E-00	0.11114 E 01	
C 22008 E-00	0.48000 E-00	0.45256 E-00	0.11249 E 01	
C 23783 E-00	0.50000 E-00	0.46916 E-00	0.11357 E 01	
C 29480 E-00	0.55000 E-00	0.50977 E-00	0.11640 E 01	
C 33509 E-00	0.59999 E-00	0.54881 E-00	0.11952 E 01	
0.38840 E-00	0.65000 E-00	0.58620 E-00	0.12294 E 01	
0.44447 E-00	0.70000 E-00	0.62208 E-00	0.12661 E 01	
0.49363 E-00	0.75000 E-00	0.65600 E-00	0.13011 E 01	
0.56406 E-00	0.80000 E-00	0.69335 E-00	0.13467 E 01	
0.62860 E-00	0.84999 E-00	0.72081 E-00	0.13905 E 01	
C 69434 E-00	0.90000 E-00	0.75640 E-00	0.14365 E 01	
0.76198 E-00	0.95000 E-00	0.77960 E-00	0.14849 E 01	
0.83138 E-00	0.09999 E-01	0.80100 E-00	0.15334 E 01	
0.97508 E-00	0.10999 E-01	0.85821 E-00	0.16428 E 01	
0.11244 E 01	0.12000 E 01	0.90490 E 00	0.17585 E 01	
0.12437 E 01	0.13000 E 01	0.94760 E 00	0.18820 E 01	
0.13374 E 01	0.13999 E 01	0.97070 E 00	0.19331 E 01	
0.14000 E 01	0.15000 E 01	0.10255 E 01	0.21919 E 01	
C 17661 E 01	0.16000 E 01	0.10554 E 01	0.22979 E 01	
C 19354 E 01	0.16999 E 01	0.10858 E 01	0.24509 E 01	
0.21C77 E 01	0.17999 E 01	0.11139 E 01	0.26109 E 01	
0.22829 E 01	0.19000 E 01	0.11139 E 01	0.27778 E 01	
0.24666 E 01	0.20000 E 01	0.11641 E 01	0.29515 E 01	
C 26441 E 01	0.20999 E 01	0.11866 E 01	0.31318 E 01	
0.28191 E 01	0.21999 E 01	0.12076 E 01	0.33188 E 01	
0.30087 E 01	0.30000 E 01	0.12472 E 01	0.34246 E 01	
C 31960 E 01	0.23999 E 01	0.12455 E 01	0.37125 E 01	
C 33885 E 01	0.24999 E 01	0.12628 E 01	0.39191 E 01	
0.35771 E 01	0.26000 E 01	0.12790 E 01	0.41321 E 01	
0.37707 E 01	0.27000 E 01	0.12942 E 01	0.43517 E 01	
C 39665 E 01	0.27999 E 01	0.13087 E 01	0.45574 E 01	
0.41642 E 01	0.28999 E 01	0.13223 E 01	0.48097 E 01	
0.43639 E 01	0.30000 E 01	0.13352 E 01	0.50482 E 01	
0.45456 E 01	0.30999 E 01	0.13474 E 01	0.52532 E 01	
0.47691 E 01	0.19999 E 01	0.13572 E 01	0.54544 E 01	
0.49745 E 01	0.32999 E 01	0.13700 E 01	0.58019 E 01	
0.51818 E 01	0.34000 E 01	0.14005 E 01	0.60657 E 01	
0.53908 E 01	0.34999 E 01	0.13904 E 01	0.63360 E 01	
0.56C19 E 01	0.35999 E 01	0.14000 E 01	0.66121 E 01	
0.58146 E 01	0.37000 E 01	0.14091 E 01	0.68947 E 01	
0.60291 E 01	0.38000 E 01	0.14177 E 01	0.71835 E 01	
0.62454 E 01	0.38999 E 01	0.14261 E 01	0.74785 E 01	
0.64600 E 01	0.40000 E 01	0.14374 E 01	0.76900 E 01	
0.67127 E 01	0.39999 E 01	0.14560 E 01	0.87210 E 01	
0.67579 E 01	0.45000 E 01	0.14693 E 01	0.93794 E 01	
0.82682 E 01	0.47999 E 01	0.16874 E 01	0.10413 E 02	
0.87356 E 01	0.49999 E 01	0.14984 E 01	0.11134 E 02	
0.94485 E 01	0.52999 E 01	0.15136 E 01	0.12220 E 02	
0.99314 E 01	0.55000 E 01	0.15229 E 01	0.13043 E 02	
C 10667 E 02	0.57999 E 01	0.15157 E 01	0.14262 E 02	
0.11164 E 02	0.59999 E 01	0.15437 E 01	0.15156 E 02	
0.14662 E 02	0.59999 E 01	0.15511 E 01	0.15972 E 02	
0.13213 E 02	0.67999 E 01	0.15712 E 01	0.18729 E 02	
0.13738 E 02	0.70000 E 01	0.15772 E 01	0.19697 E 02	
C 15077 E 02	0.74799 E 01	0.15909 E 01	0.22222 E 02	
0.16447 E 02	0.80000 E 01	0.16031 E 01	0.24902 E 02	
0.17284 E 02	0.82999 E 01	0.16097 E 01	0.26583 E 02	
0.17849 E 02	0.84999 E 01	0.16119 E 01	0.27773 E 02	
0.18418 E 02	0.86999 E 01	0.16180 E 01	0.28911 E 02	
0.19474 E 02	0.88999 E 01	0.16237 E 01	0.30462 E 02	
0.20742 E 02	0.90000 E 01	0.16275 E 01	0.33862 E 02	
0.22723 E 02	0.09999 E 01	0.16452 E 01	0.37156 E 02	
0.25295 E 02	0.11000 E 02	0.16544 E 01	0.44204 E 02	
0.28462 E 02	0.12000 E 02	0.16642 E 01	0.51867 E 02	
0.31730 E 02	0.13000 E 02	0.16762 E 01	0.60143 E 02	
0.35094 E 02	0.13999 E 02	0.16850 E 01	0.69032 E 02	
0.38548 E 02	0.15000 E 02	0.16926 E 01	0.78535 E 02	
0.42490 E 02	0.16000 E 02	0.16993 E 01	0.88532 E 02	
0.45423 E 02	0.17000 E 02	0.17075 E 01	0.98662 E 02	
0.49423 E 02	0.18000 E 02	0.17105 E 01	0.11072 E 03	
0.53208 E 02	0.19000 E 02	0.17153 E 01	0.12268 E 03	
0.57068 E 02	0.20000 E 02	0.17196 E 01	0.13525 E 03	
0.61C01 E 02	0.20999 E 02	0.17236 E 01	0.14843 E 03	
0.65502 E 02	0.22000 E 02	0.17271 E 01	0.16225 E 03	
0.73212 E 02	0.23999 E 02	0.17334 E 01	0.19169 E 03	
0.81684 E 02	0.26000 E 02	0.17388 E 01	0.22577 E 03	
0.90400 E 02	0.27999 E 02	0.17434 E 01	0.25791 E 03	
0.98449 E 02	0.29999 E 02	0.17480 E 01	0.29472 E 03	
0.14727 E 03	0.40000 E 02	0.17617 E 01	0.51551 E 03	
0.19985 E 03	0.50000 E 02	0.17703 E 01	0.79762 E 03	
0.28603 E 03	0.65000 E 02	0.17784 E 01	0.13357 E 04	
0.37974 E 03	0.80000 E 02	0.17635 E 01	0.20119 E 04	
-0.47998 E 03	0.95000 E 02	0.17870 E 01	0.28260 E 04	
0.51471 E 03	0.09999 E 03	0.17879 E 01	0.31281 E 04	
0.62225 E 03	0.11499 E 03	0.17901 E 01	0.34669 E 04	
0.68446 E 03	0.12000 E 03	0.17931 E 01	0.52632 E 04	
0.85308 E 03	0.14500 E 03	0.17934 E 01	0.65349 E 04	
b 0.97506 E 03	0.16000 E 03	0.17946 E 01	0.79484 E 04	

a Read as 0.22407×10^{-1} .

b Read as 0.17506×10^3 .

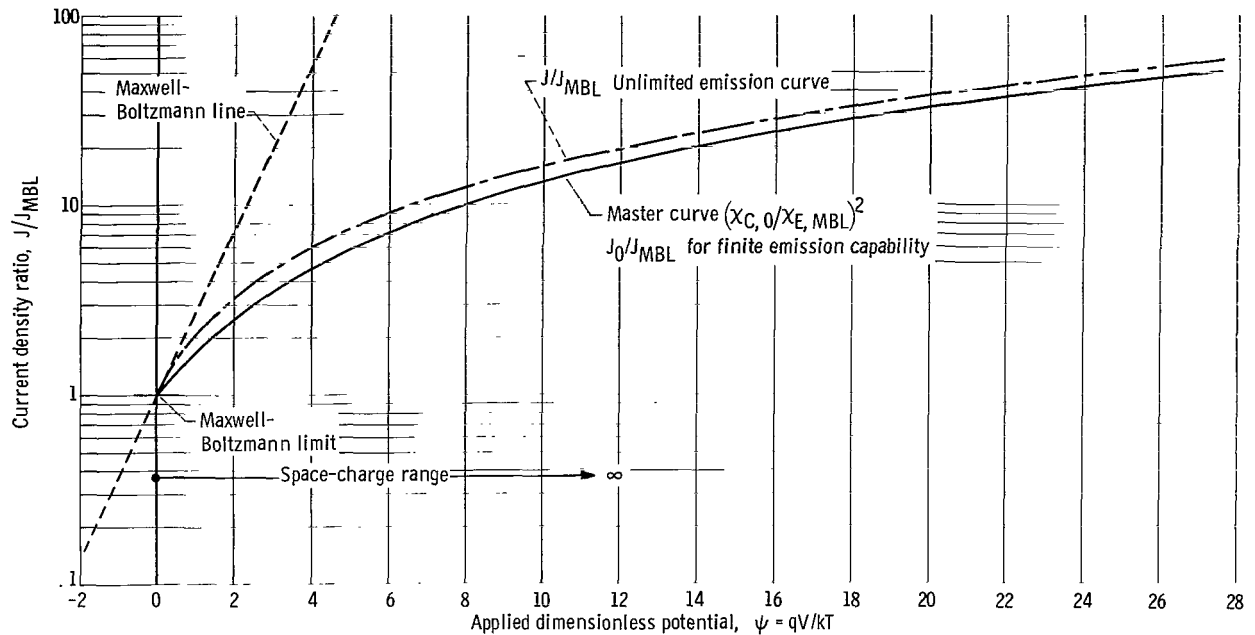


Figure IV:3. - Space-charge curves used in analysis of current-voltage data from planar diodes.

going from the Maxwell-Boltzmann limit to saturation $\psi_{E,MBL} + \psi_{C,0}$ is uniquely determined. These functional relations are useful in treating experimental data and have been compiled in table IV:1. Knowledge of any one of the terms, $\chi_{E,MBL}$, $\chi_{C,0}$, $\chi_{C,0}^2/\chi_{E,MBL}^2$, or $\psi_{E,MBL} + \psi_{C,0}$, uniquely determines all other quantities. It should be noted that $\chi_{C,0}^2/\chi_{E,MBL}^2$ is equivalent to J_0/J_{MBL} and also $\psi_{E,MBL} + \psi_{C,0}$ corresponds to the difference in applied potential (in dimensionless volts) that exists between the Maxwell-Boltzmann limit and the saturation condition. A convenient manner to present the unique relation of the current voltage in the space-charge region is shown in figure IV:3 where the logarithm of J_0/J_{MBL} is plotted as a function of applied potential $\psi_{E,MBL} + \psi_{C,0}$ (solid line). Included in the plot is the straight line (dashed) representation of the Maxwell-Boltzmann line and an unlimited emission curve (dashed line) that will be discussed in section VI. The solid line is the master curve discussed by Nottingham in reference 2. The utility of the master curve is that, with a minimum of experimental information, it permits the quick establishment of the relations between J_{MBL} , J_0 , and the applied voltage difference and also provides a starting point for a more detailed treatment of space-charge theory.

V - APPLICATION OF MASTER CURVE

Graphical solutions of space-charge relations are achieved with the "master curve" by plotting the experimental current-voltage data as the logarithm of the current against dimensionless volts on a separate sheet in scales self-consistent with figure IV:3. (The use of dimensionless volts implies knowledge of emitter temperature, which can be determined from the slope of the Maxwell-

Boltzmann line (eq. II:2) or from direct measurement). The master curve then is shifted so that the Maxwell-Boltzmann limits coincide and coordinates of the two sheets are parallel (transparent master graphs or templates are quite useful for this purpose). The current is now normalized in the ratio form in terms of the ordinate of the master curve. The experimental curve must intercept the master curve at the unique condition of zero field at the emitter if space-charge behavior exists. Thus J_0 and related quantities such as work function can be established. The ratio of J_0/J_{MBL} or the dimensionless potential interval $\psi_{E,MBL} + \psi_{C,0}$ can be used to identify $x_{E,MBL}$ and $x_{C,0}$ through table IV:1.

The effective spacing can be determined from $x_{E,MBL}$ or $x_{C,0}$ and equation (III:2) since T , J_{MBL} , and J_0 are also known. As stated previously, figure III:1 (p. 7) graphically relates x , w , and emitter temperature for both ions and electrons and thus is convenient for determining spacing.

Reiterating, two procedures exist by which the saturation current can be determined from the current at the Maxwell-Boltzmann limit. The first requires knowledge of J_{MBL} , T , and w that corresponds to $x_{E,MBL}$; this in turn defines the ratio of J_0/J_{MBL} as given in figure III:1. Other relations such as $x_{C,0}$ and $\psi_C + \psi_E$ are found directly in table IV:1 by entering at J_0/J_{MBL} or $x_{E,MBL}$. An alternate procedure does not require knowledge of spacing but requires that the experimental current-voltage data possess a saturation behavior at a distance equal to the distance that exists when the Maxwell-Boltzmann limit is determined. An intercept technique based on transposing actual data on the theoretical curve provides a solution to the space-charge relations. Once the two end points of the space-charge region are established, transition curves of current-voltages between the end points can be determined. This is the subject of the next section.

VI - TRANSITION CURVES IN SPACE-CHARGE REGION

If it is assumed that the zero field at the collector is established and that the space-charge relations govern the current-voltage behavior up to the saturation condition, it is possible to establish the entire current-voltage characteristic in the space-charge transition region for any given set of starting conditions. The method is merely an extension of the procedure given in section IV and is based upon the effect of the Boltzmann relation on transmitted current.

Returning to figure IV:1 two additional terms of use in the following analysis are the distance from the emitter surface to the space-charge minimum x_M and the corresponding distance to the collector x_N . Then

$$w = x_M + x_N$$

As before, the potential in the emitter space is described by

$$x_E = f(\psi_E) \quad (VI:1)$$

(e.g., table III:1(a), p. 7) and in the collector space

$$x_C = f(\psi_C) \quad (\text{VI:2})$$

(e.g., table III:1(b), p. 7). In the region where the space-charge minimum is in the interelectrode space, the dimensionless distance is

$$x_{E,M} + x_{C,N} = \frac{KJ^{1/2}x_M}{T^{3/4}} + \frac{KJ^{1/2}x_N}{T^{3/4}} \quad (\text{VI:3})$$

Also

$$x_{E,M} + x_{C,N} = \frac{KJ_{MBL}^{1/2}(x_M + x_N)}{T^{3/4}} \exp\left(\frac{\psi_{E,MBL} - \psi_{E,M}}{2}\right) \quad (\text{VI:4})$$

(refer to fig. IV:1 for an example of the dimensionless potential distribution). Since $x_M + x_N = w$,

$$x_{C,N} = \left[x_{E,MBL} \exp\left(\frac{\psi_{E,MBL} - \psi_{E,M}}{2}\right) \right] - x_{E,M} \quad (\text{VI:5})$$

or

$$\underbrace{f(\psi_{C,N})}_{\text{eq. (VI:2)}} = \left[x_{E,MBL} \exp\left(\frac{\psi_{E,MBL} - \psi_{E,M}}{2}\right) \right] - \underbrace{f(\psi_{E,M})}_{\text{eq. (VI:1)}} \quad (\text{VI:6})$$

Equation (VI:6) is sufficient to solve the entire space-charge transition curve for any initial value of $x_{E,MBL}$. The procedure is tedious since it involves (1) starting with a given $x_{E,MBL}$ and therefore $\psi_{E,MBL}$, (2) choosing space-charge barrier $\psi_{E,M}$, slightly less than $\psi_{E,MBL}$, (3) establishing the corresponding value of $x_{E,M}$, (4) solving for $x_{C,N}$, and (5) determining the value of $\psi_{C,N}$ (eq. (VI:2)).

Knowledge of $\psi_{C,N}$ for the assumed initial conditions is sufficient to establish one current-voltage point of the transition curve. The current ratio J/J_{MBL} is known from the starting conditions through the Boltzmann relation

$$\frac{J}{J_{MBL}} = \exp(\psi_{E,MBL} - \psi_{E,M}) \quad (\text{VI:7})$$

The surface potential referred to the Maxwell-Boltzmann limit is

$$\psi_{E,MBL} - \psi_{E,M} + \psi_{C,N} \quad (\text{VI:8})$$

(see fig. IV:1). The remaining points of the transition curve are found by repeating the previous process for additional incremental changes in $\psi_{E,M}$

TABLE VI:1-- LISTING OF COORDINATES FOR CURRENT-VOLTAGE TRANSITION CURVES IN SPACE-CHARGE REGION

Current density ratio, J/J_{MBL}	Dimensionless distance at MBL, $X_{E,MBL}$																		
	0.2	0.3	0.4	0.5	0.6	0.7	0.8	0.9	1.0	1.1	1.2	1.3	1.4	1.5	1.6	1.7	1.8	b 1.806	
Surface potential referenced to MBL, $\psi_{E,0} - \psi_{E,M} + \psi_{C,N}$																			
a _{1.1}			0.1184	0.1088	0.1048	0.1026	0.1013	0.1005	0.1000	0.09964	0.09942	0.09927	0.09918	0.09913	0.09911	0.09919	0.09920		
a _{1.158}			.273																
a _{1.2}				.2554	.2240	.2122	.2060	.2024	.2002	.1987	.1978	.1972	.1968	.1966	.1966	.1967	.1967		
a _{1.242}				.4093															
a _{1.3}					.3768	.3328	.3155	.3062	.3008	.2973	.2952	.2938	.2930	.2926	.2925	.2927	.2927		
a _{1.36}						0.5857													
a _{1.4}							0.4742	0.4318	0.4127	0.4021	0.3957	0.3918	0.3894	0.3880	0.3873	0.3870	0.3872		
a _{1.52}							.8130												
a _{1.6}								.7044	.6375	.6084	.5924	.5831	.5776	.5744	.5728	.5722	.5725		
a _{1.74}									1.1077										
a _{1.8}										0.8914	0.8224	0.7902	0.7726	0.7625	0.7568	0.7540	0.7529		
a _{2.0}										1.232	1.050	.9904	.9608	.9446	.9357	.9313	.9296	.9300	
a _{2.07}											1.495								
a _{2.2}												1.301	1.195	1.148	1.124	1.111	1.105		
a _{2.4}												1.609	1.406	1.336	1.302	1.284	1.276		
a _{2.54}												2.019							
a _{2.6}													1.628	1.525	1.478	1.455	1.444	1.440	
a _{2.8}													1.867	1.715	1.653	1.623	1.609	1.604	
a _{3.0}													2.139	1.908	1.827	1.790	1.772	1.766	
a _{3.25}													2.755						
a _{3.50}													2.410	2.259	2.198	2.170	2.161	2.161	
a _{4.00}													2.976	2.691	2.596	2.557	2.543	2.543	
a _{4.44}													3.845						
a _{4.50}														3.128	2.988	2.934	2.916	2.915	
a _{5.00}														3.575	3.374	3.303	3.278	3.277	
a _{5.5}														4.4045	3.756	3.664	3.633	3.631	
a _{6.0}														4.561	4.134	4.018	3.981	3.978	
a _{6.61}														5.599					
a _{7.0}															4.887	4.709	4.657	4.652	
a _{8.0}															5.644	5.381	5.310	5.304	
a _{9.0}															6.420	6.057	5.944	5.935	
a _{10.0}															7.249	6.879	6.562	6.550	
a _{11.0}															8.269	7.311	7.165	7.150	
a _{11.3}															8.804				
a ₁₂																7.933	7.755	7.736	7.736
a ₁₄																9.156	8.900	8.873	8.873
a ₁₆																10.36	10.00	9.969	9.970
a ₂₀																12.79	12.12	12.06	12.06
a _{24.2}																16.07			
a ₂₅																	14.62	14.53	14.53
a ₃₀																	17.00	16.86	16.87
a ₄₀																	21.45	21.24	21.25
a ₅₀																	25.72	25.33	25.33
a ₆₀																	29.79	29.19	29.19
a ₈₀																	37.75	36.41	36.41
a _{89.5}																	42.45		
a ₁₀₀																		43.12	43.13
a ₁₅₀																		58.40	58.41
a ₂₀₀																		72.22	72.23
a ₂₅₀																		85.04	85.04
a ₃₀₀																		97.09	97.10
a ₄₀₀																		119.5	119.5
a ₅₀₀																		140.3	140.3

^aDenotes intercept with master curve.^bUnlimited emission condition as calculated by eq. (VII:1).

until the limit, where $\psi_{E,MBL} - \psi_{E,M} = 0$, and thus saturation conditions are obtained.

Numerical solutions of the transition curves (i.e., typical current-voltage curves in the space-charge region) have been determined and are listed in table VI:1. The intervals are sufficient for the determination of most space charge dominated current-voltage characteristics. The ratio of J/J_{MBL} and the corresponding value of surface potential difference ($\psi_{E,MBL} - \psi_{E,M} + \psi_{C,M}$) are presented for the range of $x_{E,MBL}$ (current density, temperature, spacing, and charge to mass ratio) of usual interest in space-charge solutions.

VII - LIMITING SPACE-CHARGE CURVE

A result of interest with regard to the current-voltage transition curves is the similarity of the current ratio J/J_{MBL} and applied potential for those conditions where $x_{E,MBL}$ approaches 1.806. If table III:1(a) (p. 7) or figure III:2 (p. 9) are referred to, it can be seen that, at values of $\psi_E > 10$, x_E is nearly to the limiting value (1.799 compared to 1.806). For all practical purposes over the range of voltages for which $\psi_{E,MBL}$ is greater than 10, the current across the diode is independent of the emission capability of the emitter. Surface barriers are suppressed, space charge dominates, and the emitter acts as if it possesses unlimited emission capability.

When $\psi_{E,MBL}$ is greater than 10, the assumption that $x_{E,MBL}$ is nearly equal to 1.806 permits the description of the transition curves by the following approximation of equation (VI:6):

$$f(\psi_{C,N}) \approx 1.806 \left[\exp \left(\frac{\psi_{E,MBL} - \psi_{E,M}}{2} \right) \right] - 1.806 \quad (\text{VII:1})$$

This approximation is based upon the following:

- (1) When $\psi_{E,MBL} > 10$, $x_{E,MBL} \approx 1.806$.
- (2) Also, $x_{E,M} \approx 1.806$ at $\psi_{E,M}$ near 10.
- (3) At the lower values of $\psi_{E,M}$, $\left[\exp \left(\frac{\psi_{E,MBL} - \psi_{E,M}}{2} \right) \right] \gg x_{E,M}$.

Then

$$\exp (\psi_{E,MBL} - \psi_{E,M}) = \frac{J}{J_{MBL}} \quad (\text{VII:2})$$

The ratio of J/J_{MBL} as a function of change in applied potential from the MBL limit ($\psi_{E,MBL} - \psi_{E,M} + \psi_{C,M}$) may be determined directly. This result is tabulated in the last column in table VI:1 and corresponds to the curve labeled unlimited emission in figure IV:3 (p. 15). The unlimited emission curve provides an adequate representation of the current-voltage regions for space-charge

limited current conditions over a wide range of applied potentials and accurately reflects the current-voltage trends during the initial application of accelerating potential for almost all cases where space-charge effects are of significance.

VIII - REMARKS CONCERNING APPLICATION OF SPACE-CHARGE THEORY

It is generally impossible to separate the electron current from the ion current so that the Maxwell-Boltzmann limit for the ion current is quantitatively established. Only in extreme cases of high ion current density and a minimum of collision phenomena is the match between theory and experiment satisfactory. A more applicable space-charge treatment of ion current deals with the determination of the applied voltage needed to reach ion saturation at the condition before the onset of the Schottky effect. The procedure requires a reasonable estimate of the saturated ion current J_0 . In general, this is calculated by knowing the arrival rate of cesium atoms, cesium ionization potential, and the estimated or measured emitter work function. The Langmuir-Saha equation or some modification of it may be used to calculate the anticipated zero-field ion current density. The value of the constant K (eq. (III:2)) is 1.442×10^7 for the case of cesium ions. If this value is used along with the other data in equation (III:2) or figure III:1 (p. 6), the value of $x_{c,0}$ may be computed. Reference to table III:1(b) (p. 7) establishes the corresponding value of $\psi_{c,0}$. This quantity when multiplied by kT/q then gives the potential difference between the surface of the emitter and the surface of the ion collector, which must be established in order to obtain the zero-field ion emission. This information coupled with the Schottky treatment of current-voltage information (to be discussed in sections IX and X) provides a useful step in analyzing current-voltage information.

The use of the generalized space-charge relations also involves the presentation of the experimental data in a form similar to the master and unlimited emission curves shown in figure IV:3 (p. 15). The procedure previously outlined required transposing the curves so that the Maxwell-Boltzmann limits coincided. The crossover of the experimental curve with the master curve gives zero-field emission and permits the direct determination of spacing w . Experiment has shown this value is in excellent agreement for the vacuum diode (ref. 2). The transition curves are also accurately described by the unlimited emission curve at the initial values of applied potentials. The plasma diode at extremely close spacing exhibits space-charge behavior in close agreement with the analytical predictions. If, however, as is true in many cases, the spacing is greater than a single mean free path for an ion or an electron, the development of plasma conditions tends to make the effective spacing considerably less than the true one. Semiquantitative information on the nature of the barrier in terms of height and location can be obtained by the use of the space-charge relations. The unlimited emission curve can also be used as a useful "barometer" of the applicability of the space-charge relations. The experimental data that clearly exceed the condition of "unlimited" data indicate the single-charge space-charge relations cannot be applied in a direct fashion and suitable adjustments must be made. The conditions in which this occurs in the case of electron transmission are often those of large ion currents. In the cases where the large ion current

predominates, application of the space charge to the ion often yields useful information enabling a sorting of electron and ion currents.

IX - GENERAL DISCUSSION OF SCHOTTKY MIRROR-IMAGE THEORY

Schottky (ref. 6) was one of the first to call attention to the mirror-image concept. The force acting on an electron as it progresses from the surface of a uniform conductor out to a point well outside of the conductor is dominated by the attraction between the electron and the induced surface charge of the opposite sign distributed over the conducting surface. This statement implies that the outside space is electrostatically field-free except for the field produced by the electron or ion and its induced surface charge.

Figure IX:1 has been prepared to give an accurate scale drawing of the mirror-image potential function. Two curves are shown. The upper curve is the potential function for an electron, and the lower curve is the potential function for a positive ion. In both cases the mirror-image force is one which attracts the electron or ion to the surface. Thus, electron energy levels lie in this potential-function plane below the electron potential function line; ion energy levels lie above the potential function.

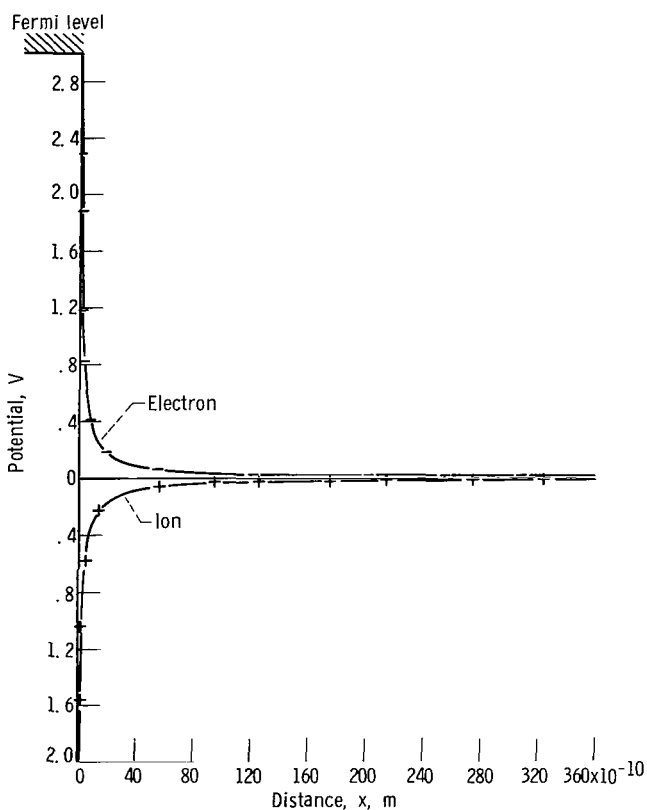


Figure IX:1. - Mirror-image potential function for electrons and singly charged ions.

Some ambiguity exists in the point of termination of the mirror-image potential function. Figure IX:1 indicates intersection at the Fermi level for the electron image function. The ion image function is considered to be symmetrical with respect to the electron image function. The axis of symmetry is the zero potential line.

Figure IX:1 displayed the electron and ion functions in the absence of any external electrostatic field produced by surface and/or space charges. The superposition of electrostatic forces and the mirror-image forces permits the display of potential functions in the presence of combined forces. Figure IX:2 illustrates the superposition and has been prepared to show two important facts. The first relates to the potential functions with zero external field. The ordinate scale has been expanded a factor of 10 to show that at a distance of 1.4×10^{-8} meter, the potential function differs from that at infinity by only 0.026 electron volt. This energy is the electron

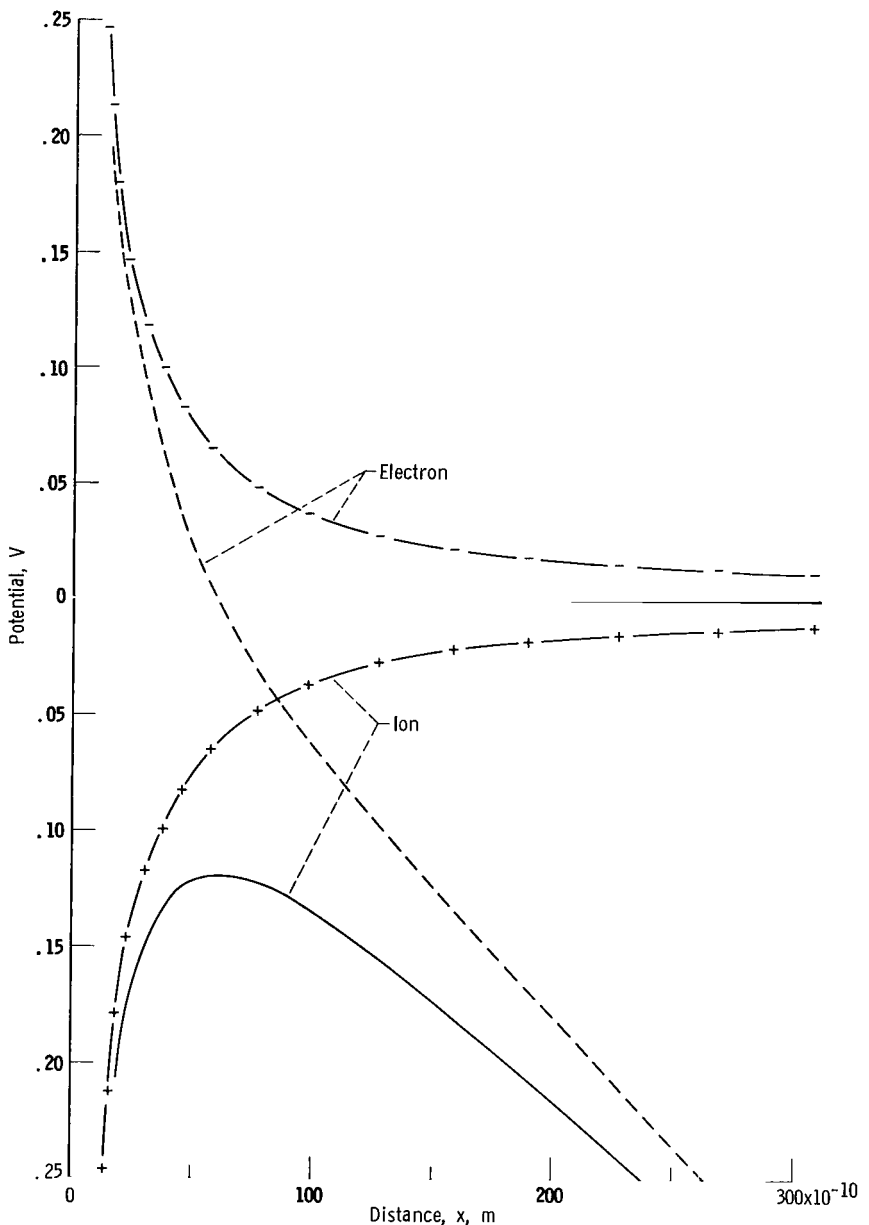


Figure IX:2. - Mirror-image potential functions in presence of ion accelerating field of 10^7 volts per meter.

volt equivalent of room temperature. Thus, for all practical purposes, the mirror-image force is of little or no consequence at a distance from the conducting surface of 10^{-8} meter (approximately 40 to 100 atomic radii).

The second fact relates to the potential functions associated with an ion accelerating field of 10^7 volts per meter. Again, all ion energy levels lie above the ion potential line, shown here as a solid line. Similarly, the electron energy levels all lie below the electron potential line shown as the dashed line. Ion removal from the surface is enhanced by the accelerating field. The

critical distance for ion escape has been brought to approximately 0.6×10^{-8} meter, and the necessary initial kinetic energy for escape has been lowered by 0.12 electron volt. (The effects are identical for electrons in the presence of an electron accelerating field). The atomic scale of the dimensions involved in the location of the critical distance and point of the termination of the mirror-image function permits the simple superposition of the Schottky effect on the thermionic emission, the space charge, and the sheath relations treated in this report. The relations that follow are limited to accelerating fields of 10^7 volts per meter or less. Field strengths greater than this introduce a probability of electron tunneling and are also more dependent on the nature of the force function near the emitter surface. Morris (ref. 7) has analyzed Schottky (and penetration) effects on electron emission for a mirror-image function terminating on the conductor surface at the Fermi level. The comparison (ref. 7) of the terminated image function to the more usual simple nonterminated form indicates that, at field strengths less than 10^7 volts per meter, the current densities of the two cases deviate by only 1 percent. Field strengths greater than 10^7 volts per meter are unlikely in a thermionic converter; therefore, the simple formalism of the Schottky effect based upon the nonterminated image potential is used in the development of the equations in this section.

As a consequence of the experimental fact that both electrons and ions leave a heated surface with a Maxwell-Boltzmann energy distribution, it is possible to write the equation for the variation of current density produced by a variation in the surface field applicable to both particles. This result expressed in logarithmic form is

$$\ln J = \ln J_0 + \frac{(3.8 \times 10^{-5} E^{1/2}) 11 \ 606}{T} \quad (\text{IX:8})$$

As a first approximation it is practical to assume that the electrostatic field E is directly proportional to the difference in the surface potentials of the emitter and the collector.

The surface potential difference is determined from the applied potential by correcting for the contact potential difference (ϕ considered positive only)

$$\pm V_C = \pm(\phi_1 - \phi_2) \quad (\text{IX:9})$$

The plus sign applies for an ion accelerating field, the minus sign for an electron accelerating field. The assumption that E is proportional to the applied voltage corrected for contact potential can be expressed in terms of geometrical factor identified as the "effective spacing". This proportionality factor then appears as

$$E = \frac{V_B - (\pm V_C)}{w_{\text{eff}}} \quad (\text{IX:10})$$

where V_B (the applied potential) is treated as a positive quantity if it produces an accelerating field for the particle in question. After this substitution is made in equation (IX:8), it may be written in either of the following forms:

$$\ln J = \ln J_0 + 3.8 \times 10^{-5} \left[\frac{V_B - (\pm V_C)}{w_{\text{eff}}} \right]^{1/2} \frac{11}{T} \quad (\text{IX:11})$$

or

$$\log_{10} J = \log_{10} J_0 + 1.65 \times 10^{-5} \left[\frac{V_B - (\pm V_C)}{w_{\text{eff}}} \right]^{1/2} \frac{11}{T} \quad (\text{IX:12})$$

These equations suggest that the logarithm of the current density should be plotted as a function of the square root of the applied voltage (corrected for contact potential difference) divided by the electron volt equivalence of temperature. If a straight line results, it is then justified to assume that the linear relation expressed by equation (IX:10) is applicable. Field distortion which results from geometrical factors only does not interfere with the linearity of the plot but simply gives an unrealistic value of w_{eff} . Space-charge effects are the most serious and the most difficult to include in the analysis since then E will be a nonlinear function of V . If the space charge is due to the ions or electrons being measured, the field itself will always be weaker than that computed from geometrical considerations. If the space-charge present is of the opposite sign, then the field will be stronger than would be computed by equation (IX:10). Both of these effects become less important at higher values of applied voltage. This can be seen in figure IX:3, which is a typical "Schottky plot" of cesium ion emission observed in a thermionic converter operating at voltages corresponding to a strong ion accelerating field. It is legitimate to apply equation (IX:12) to data of this type by drawing a straight line

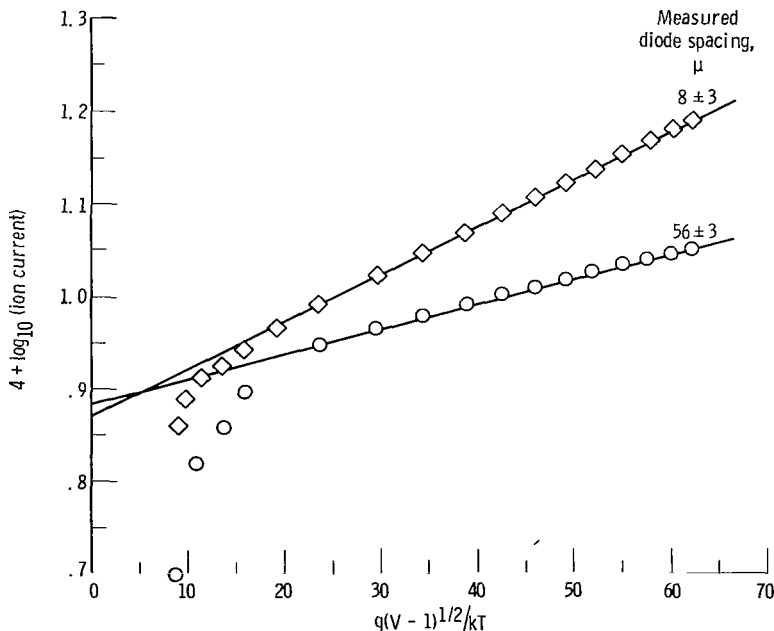


Figure IX:3. - Typical Schottky plot of cesium ion emission from tungsten emitter in planar thermionic converter. Emitter temperature, 1472° K; cesium reservoir temperature, 470° K; $\varphi_1 - \varphi_2 \approx 1$.

through the higher voltage data and extrapolating the line to zero voltage (based on surface potential difference). The value of $\log_{10} J$ is thus established. The slope of the line gives the value of spacing. This may be expressed explicitly as

$$w_{\text{eff}} = \frac{2.72 \times 10^{-10}}{S^2} \text{ m} \quad (\text{IX:13})$$

In this equation, S is the slope of the straight line drawn when $\log_{10} J$ is used; that is,

$$S = \frac{T}{11,606} \frac{\log_{10} J_1 - \log_{10} J_2}{\sqrt{V_1 - (\pm V_C)} - \sqrt{V_2 - (\pm V_C)}} \quad (\text{IX:14})$$

X - CONCLUDING REMARKS CONCERNING USE OF SCHOTTKY THEORY

Although the theory reviewed in the previous section of this report has generally been applied to electrons, it is equally valid as it applies to ions. The theory is most likely to be of value in the treatment of ion currents in the analysis of voltage-current curves taken in a plasma diode. When the ratio of the emitter temperature to the cesium bath temperature is less than 2.9, the sheath condition at the emitter is generally electron rich. Ion current data taken in a very closely spaced diode and with applied potentials approximately 2 volts more negative than the open-circuit voltage in this electron-rich region follow the Schottky theory quite well. The slopes are very consistent with the actual spacing. The extrapolation of the line to establish the zero-field condition yields information by which a comparison can be made with the Langmuir-Saha theory of ionization. This method of analysis applied to spacings that are large compared with the mean free path of the ions often results in a nearly straight line display of the data, and yet the slope of the line is far in excess of that anticipated from geometrical considerations. Thus an abnormally small value of w_{eff} in comparison with the actual value is interpreted as a direct indication that a "plasma" or "collisional" condition has developed in the interelectrode space. The field is no longer directly proportional to the applied voltage but is greatly distorted by the presence of space-charge and collisional effects. The observed current falls very much more rapidly with a change in voltage and therefore corresponds to a much steeper slope of the Schottky line than can possibly be justified on the Schottky theory basis. Such an analysis still has value in that the experimental results cast in this form clearly illustrate that the flow of ions is inhibited by the presence of the atoms in spite of the fact that an ion accelerating field is presumed to exist across the entire interelectrode space.

The Maxwell-Boltzmann portion of the log - current-voltage curve is usually linear over several orders of magnitude of current flow in a well-controlled vacuum diode experiment. Subsequent interpretation of the space-charge region leading to the determination of emitter and collector work function is quite direct by the techniques described in the earlier sections of this report. The presence of ion currents even though small distorts the Boltzmann line and in-

terferes with the "single-charge" interpretation of the net current results. A first step in the reduction of the net current data (where $+J \ll -J$) is the use of the Schottky analysis to determine the zero-field ion current. If this value and other terms in χ indicate the ion space-charge effect is minor, then the net current can be corrected directly for the ion current contribution. As the accelerating potential is reduced and the simple corrections become more inaccurate, the large electron current will usually dominate and mask the uncertainties in reflection and space-charge effects on ion currents.

XI - REVIEW OF SHEATH AND PLASMA THEORY OF ISOTHERMAL DIODE

Voltage-current curves of a cesium plasma diode operated at extremely close spacing are quite readily interpreted in terms of conventional formulations based on the Richardson-Dushman emission equation, Langmuir-Saha (ref. 8) ion production probability equation, conventional space-charge theory, Schottky (ref. 6) theory, and extrapolation of Langmuir-Taylor (ref. 9) cesium coverage data. It is particularly interesting to observe both the ion and electron currents at various spacings when the emitter temperature T and the cesium temperature T_{Cs} are related in terms of their ratio by $2.9 < (T/T_{Cs}) < 3.4$. Within this range, conditions near the emitter go from electron rich to ion rich. It is assumed that under the latter condition, there is no difficulty collecting the full value of electron emission current available at the emitter. Experiment shows that over a limited range in spacing, this full current is observed, but as the spacing is increased to become comparable with the electron mean free path an electron space-charge barrier develops to inhibit the flow in spite of the ion-rich condition near the surface (ref. 10). The reverse of this picture applies if the emitter sheath is electron rich. The ion production observed at larger spacings often falls below that observed at close spacings. In both cases, it is believed that a plasma condition has formed close to the emitter and that variations in applied collector potential modify the collector sheath more noticeably than they do the electron- or ion-limiting barriers. In recognition of this observation the theory of the isothermal diode was analyzed in detail (ref. 11) so that information on the potentials associated with the plasma could be established. A brief review of the results of the isothermal analysis is included to show how the numerical results were established. Inasmuch as the equations and their derivations are readily found in the literature, the emphasis of the following sections will be placed upon presenting the equations in a form that permits quick application to experimental data. The relations involving numerical values of cesium vapor pressure differ from those in reference 11 since more recent vapor pressure data are used.

The first step in the development of the theory of an isothermal diode comes from an application of the Saha (refs. 8 and 12) equation, which relates the concentration of ions or electrons (since these are equal) to the temperature, concentration of atoms, and the ionization potential. This equation is

$$+n_p = -n_p = \left[\frac{2(2\pi mkT)^{3/2}}{h^3} \frac{n}{2} \exp\left(\frac{qV_i}{kT}\right) \right]^{1/2} (1-f)^{1/2} \quad \text{no./m}^3 \quad (\text{XI:1})$$

The random current for cesium ions is directly expressible by

$$\ln +J_P = -17.51 + \frac{5}{4} \ln T - \frac{qV_i}{2kT} + \frac{1}{2} \ln n \quad \text{amp/sq m} \quad (\text{XI:2})$$

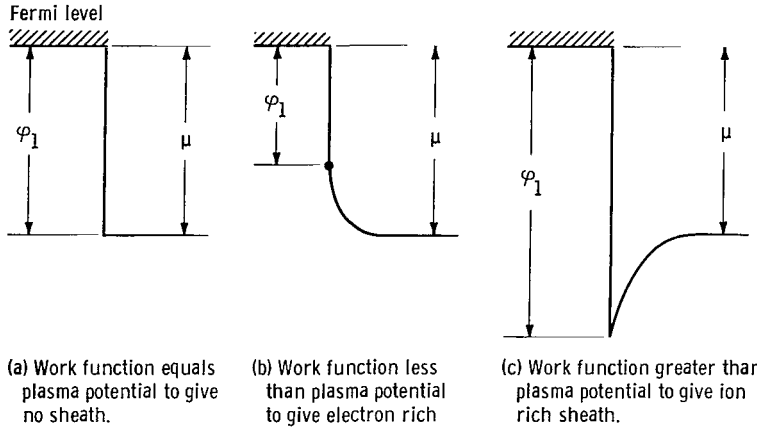


Figure XI:1. - Examples of potential diagrams for three different work functions.

The random current of electrons is given by

$$\ln J_p = -11.31 + \frac{5}{4} \ln T - \frac{qV_i}{2kT} + \frac{1}{2} \ln n \quad \text{amp/sq m} \quad (\text{XI:3})$$

These two current densities are related by the square root of mass ratio (492) for cesium.

An isothermal plasma is generally bounded by a material substance in which it is possible to identify the Fermi level. As a result of the definition of chemical potential (e.g., ref. 13) and the use of equation (XI:2), the plasma potential, relative to the Fermi level of the surrounding material, is given by

$$\mu = \frac{kT}{q} \left(25.31 + \frac{3}{4} \ln T + \frac{qV_i}{2kT} - \frac{1}{2} \ln n \right) \quad \text{v} \quad (\text{XI:4})$$

The diagrams of figure XI:1 illustrate three examples. The first is the potential diagram associated with the absence of any plasma sheath found when the work function is equal to the plasma potential. In figure XI:1(b), the work function is lower while figure XI:1(c) applies to a high work-function surface. In each case, the electron emission from the surface is equal to the electron current impinging on the surface from the plasma. The net electron current at the boundary and any position in the sheath is always zero. The net ion current at the boundary and in the sheath is also always zero.

Since diodes for the thermionic conversion of heat to electricity are never isothermal, the application of the aforementioned results is somewhat qualitative; thus there is seldom any need to determine the isothermal plasma potential to an accuracy better than about 1 percent. Figure XI:2 serves to relate the plasma potential to the isothermal temperature and the cesium atom density expressible in terms of the corresponding cesium condensation temperature. For more accurate results, a very simple formula may be used with the help of the correlation chart given as figure XI:3. Both approaches are based on non-collisional transport in the interelectrode space. The equation to be used

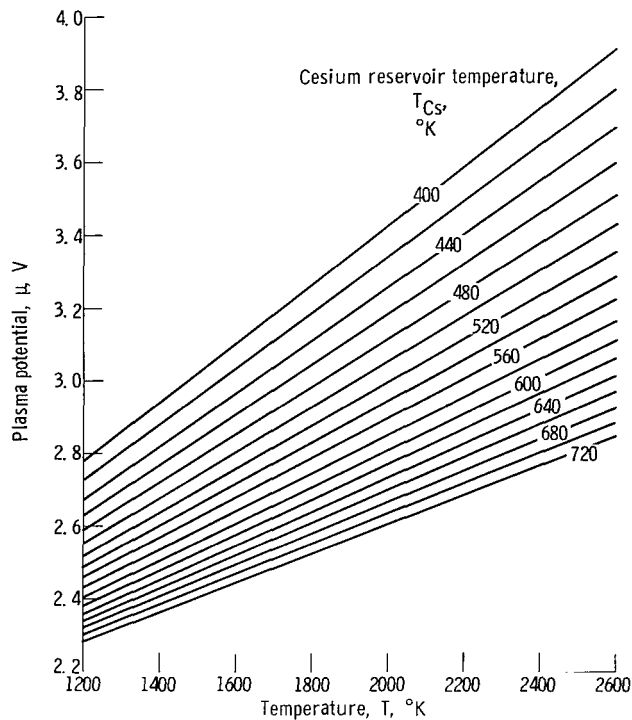


Figure XI:2. - Plasma potential as function of surface temperature and cesium reservoir temperature.

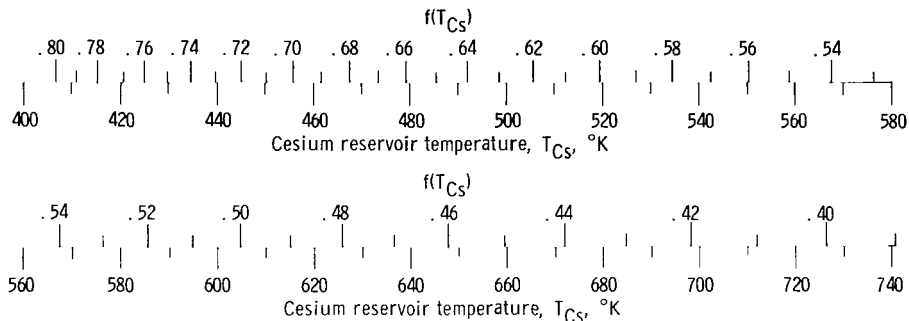


Figure XI:3. - Correlation chart for $f(T_{CS})$ as function of cesium reservoir temperature used in equation (XI:6) ($\mu = 1.799 + f(T_{CS})T \times 10^{-3}$, V) for computation of isothermal plasma potential referenced to Fermi level.

with this chart is

$$\mu = 1.799 + f(T_{CS}) \frac{T}{1000} \quad V \quad (\text{XI:6})$$

XII - FOWLER POTENTIAL FUNCTION IN SHEATH

The Fowler (ref. 14) solution of the space-charge equation is used to give a determination of the distribution in potential in the transition region between the surface of the surrounding conductor and the plasma potential μ . Figure XII:1 defines certain essential points. The mathematical solution allows

the potential to approach a value of ∞ by assuming a "fictitious" surface which lies inside the true surface a distance x_0 . The detailed development of the equations in this section is given in reference 11. The Fowler solution is simplified by the introduction of a distance parameter similar to the "Debye distance"; the Fowler distance differs only by a factor. This parameter is given by

$$x_1 = \frac{1}{2} \frac{(\epsilon_0 k)^{1/2}}{q} \frac{T_1^{1/2}}{n_p^{1/2}} = 34.5 \frac{T_1^{1/2}}{n_p^{1/2}} \quad \text{m or } 5 \times 10^{-3} \text{ Debye lengths} \quad (\text{XII:1})$$

The exact equation for the distance from the fictitious surface to the real surface is given by

$$x_0 = x_1 \sqrt{2} \ln \left(\tanh \left| \frac{\varphi_1 - \mu}{\frac{4kT}{q}} \right| \right)^{-1} = x_1 \sqrt{2} \ln \left(1 + \frac{2}{\exp \left| \frac{2kT}{q} \right| - 1} \right) \quad \text{m} \quad (\text{XII:2})$$

The insertion of realistic values into equation (XII:2) shows that x_0 seldom deviates from x_1 as much as a factor of 2. A specific numerical illustration may be of interest as it applies to the temperature ratio T_1/T_{Cs} of $2200^\circ \text{K}/660^\circ \text{K}$, which yields a value of x_1 of 1.42×10^{-7} meter. The corresponding values of φ_1 and μ are 3.18 and 2.83 volts, respectively. With these values substituted in equation (XII:2), the value of x_0 is 1.68×10^{-7} meter, which is only 20 percent larger than x_1 .

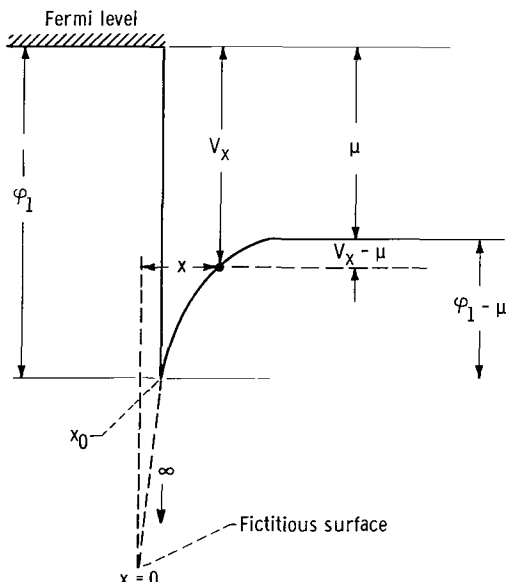


Figure XII:1. - Potential diagram for positive ion sheath.

The Fowler space-charge equation expressed in terms of the potential function V_x relative to the isothermal plasma potential is given by

$$V_x - \mu = \frac{4kT}{q} \tanh^{-1} \left[\exp \left(-\frac{x}{\sqrt{2} x_1} \right) \right] \quad \text{v} \quad (\text{XII:3})$$

This equation may be solved to give the distance x from the fictitious surface to a specific value of the potential relative to the plasma potential. The equation is

$$x = x_1 \sqrt{2} \ln \left(\tanh \frac{V_x - \mu}{\frac{4kT}{q}} \right)^{-1} \quad m \quad (\text{XII:4})$$

The distance to a given value of the potential relative to the real surface requires the subtraction of x_0 (eq. (XII:2)).

It is often desirable to know the sheath thickness so that it can be compared with the actual interelectrode spacing. Inspection of equation (XII:4) shows that as V_x approaches μ , the distance x approaches infinity. This means that there is no absolutely sharp boundary to the space-charge sheath; thus some criterion should be chosen to establish a finite distance. One such practical criterion would be that $|V_x - \mu| = kT/q$ since this quantity is a good measure of thermal energy of the charged particles involved. This particular value of the distance defines the symbol $\underline{x}_{\bar{V}}$ and is given by

$$\underline{x}_{\bar{V}} = 1.99 x_1 \quad m \quad (\text{XII:5})$$

The distance from the actual surface depends on the value of x_0 given by equation (XII:2) and may be computed by

$$\underline{x}_{\bar{V}} - x_0 = x_1 \sqrt{2} \left\{ 1.407 - \ln \left[1 + \frac{2}{\exp \left(\frac{\phi_1 - \mu}{\frac{2kT}{q}} \right) - 1} \right] \right\} \quad m \quad (\text{XII:6})$$

If the difference in potential across the sheath ($\phi_1 - \mu$) is $3kT/q$ or more, the approximate form of equation (XII:6) is given by

$$\underline{x}_{\bar{V}} - x_0 \approx x_1 \sqrt{2} \left(1.407 - 2 \exp \left| \frac{\phi_1 - \mu}{\frac{2kT}{q}} \right| \right) \quad m \quad (\text{XII:7})$$

Equation (XII:2) expanded in series form is

$$x_0 = x_1 \sqrt{2} \frac{2}{\psi_1} \left(1 + \frac{1}{3 \exp \psi_1} + \frac{1}{5 \exp 2\psi_1} + \dots \right) \quad m \quad (\text{XII:8})$$

where

$$\psi_1 = \frac{\phi_1 - \mu}{\frac{kT}{q}}$$

The error in the use of only the first term of this formula is less than 1 percent for $(\phi_1 - \mu)q/kT = 3.5$; if two terms are used, the 1 percent error is at $\psi_1 = 1.5$.

The Fowler solution of the sheath analysis also establishes the field at the surface

$$\frac{d\psi_1}{d\left(\frac{x}{x_1}\right)} = \sqrt{2} \sinh \frac{\psi_1}{2} \quad (\text{XII:9})$$

In dimensional form, the field at the surface becomes

$$\frac{dV_x}{dx} = \left(\frac{2kTn_p}{\epsilon_0} \right)^{1/2} 2 \sinh \frac{\Phi - \mu}{2kT} \quad \text{v/m} \quad (\text{XII:10})$$

An approximate logarithmic form valid for $\psi_1 > 4$ is

$$\ln \left(\frac{dV_x}{dx} \right) \approx - 13.247 + \frac{1}{2} \ln n_p + \frac{1}{2} \ln T + \frac{\Phi - \mu}{2kT} \quad (\text{XII:11})$$

XIII - RELATION OF ISOTHERMAL DIODE THEORY TO SCHOTTKY REDUCTION IN WORK FUNCTION

Under some conditions of operation of practical thermionic diodes, strong ion accelerating sheaths may form which in turn increase electron emission. The increased emission may result in part from a reduction in work function in accordance with the Schottky mirror-image theory. The relations given below are based on equations in sections IX and XII and are given in a form that permit a direct calculation of "sheath" enhanced electron emission current.

A logarithmic form of equation (IX:8) is

$$\ln \ln \left(\frac{I_F}{I_0} \right) = - 10.179 + \ln \left(\frac{q}{kT} \right) + \frac{1}{2} \ln \left(\frac{dV_x}{dx} \right)_{x=x_0} \quad (\text{XIII:1})$$

In these equations, I_F is the emission current in the presence of the electron accelerating field of strength calculated by equation (XII:10) or (XII:11). The symbol I_0 is the current density from the emitter when the field is zero. This equation may be combined with equation (XII:10) to give a useful logarithmic expression as

$$\ln \left(\ln \frac{I_F}{I_0} \right) = - 14.117 + \frac{1}{4} \ln n_p + \frac{3}{4} \ln \frac{q}{kT} + \frac{1}{2} \ln \sinh \left(\frac{\Phi_1 - \mu}{2kT} \right) \quad (\text{XIII:2})$$

A second form of this equation depends on the use of equation (XII:11) in equation (XIII:1). This result, good when $(\phi_1 - \mu)/(kT/q) > 4$, is

$$\ln\left(\ln \frac{I_F}{I_0}\right) = -14.463 + \frac{1}{4} \ln n_p + \frac{3}{4} \ln\left(\frac{q}{kT}\right) + \frac{\phi_1 - \mu}{\frac{4kT}{q}} \quad (\text{XIII:3})$$

To make direct calculations from the atom density and temperature without first determining n_p , the exact and the approximate formulas are, respectively

$$\ln \ln\left(\frac{I_F}{I_0}\right) = -6.216 + \frac{9}{16} \ln\left(\frac{q}{kT}\right) - \frac{qV_i}{8kT} + \frac{1}{8} \ln n + \frac{1}{2} \ln \sinh\left(\frac{\phi_1 - \mu}{\frac{2kT}{q}}\right) \quad (\text{XIII:4})$$

For $(\phi_1 - \mu)/(kT/q) > 4$,

$$\ln \ln\left(\frac{I_F}{I_0}\right) \approx -6.562 + \frac{9}{16} \ln\left(\frac{q}{kT}\right) - \frac{qV_i}{8kT} + \frac{1}{8} \ln n + \frac{\phi_1 - \mu}{\frac{4kT}{q}} \quad (\text{XIII:5})$$

XIV - CONCLUDING REMARKS CONCERNING ISOTHERMAL DIODE THEORY

The isothermal diode theory suffers from the limitations involved in all equilibrium approaches. Its application to a thermionic converter represents a major perturbation to the basic assumptions; however, since a semiquantitative insight into the properties of a diode can be achieved from such a simple utilitarian approach, its judicious use is of value.

The exact description of the sheath region and the equations of sheath thickness and surface field have been formulated by the isothermal diode theory. The relations would be expected to give a first-order approximation of the sheath and plasma at the condition where the random current is considerably larger than the directed current. Such a condition could occur when the cesium pressure is quite high and the T_1/T_{Cs} is in the region where electron emission is modest. A similar condition can be encountered when the diode is operated with applied potential sufficiently retarded to inhibit the transmission of the electron current. Houston (ref. 15) has indicated reasonable agreement of his experimental data with isothermal theory at these conditions.

Lastly, a great deal of utility is derived from the isothermal theory in establishing some of the properties of the plasma conditions. Its use in conjunction with the space-charge theory helps to define the conditions where transitions between space-charge and plasma effects may appear in experimental results.

XV - ADDITIONAL AIDS TO ANALYSIS OF THERMIONIC CONVERTER PERFORMANCE

Continual use of the Richardson-Dushman emission equation is made in the analysis of thermionic converter data. Excellent charts exist that provide graphical solutions for these relations (see Luke (ref. 16), for example); however, the charts that are available often do not cover the range of interest in the detail desired. Presentation of comprehensive detailed charts to cover each situation involves the obvious problem of generating excess information. Therefore, a compromise has been made. Solutions to the Richardson-Dushman equation which is

$$J_0 = 1.2 \times 10^6 T^2 \exp \left(-\frac{q\phi}{kT} \right) \text{ amp/sq m} \quad (\text{XV:1})$$

in terms of the work function have been tabulated (table XV:1) for a range of current densities of 10^{-3} to 10^{-6} amperes per square meter and temperatures from 500° to 3200° K.

The exponential relation between the work function and current density permits the linear display of the tabulated results on semilog graphs in the form shown in figure XV:1. The tabulated solution provides a convenient compilation of the intercepts of each constant temperature line. Thus the user can select the range and scales of interest and quickly tailor the charts to his own use.

Cesium vapor pressure and related properties are also of primary interest in thermionic conversion. Several adequate references (refs. 17 and 18) exist and are presently in use; however, recent vapor pressure data in the 700° to 1300° K range indicate some small corrections should be made, particularly if thermodynamic consistancy is to be attained for cesium vapor in equilibrium with the liquid or solid phase. Heimel (ref. 19), in his review of the thermodynamic properties of cesium, recommends that the following equation be used for the vapor pressure of cesium:

$$\log_{10} p (\text{N/sq m}) = \frac{-4053.30}{T} - 0.915282 \log_{10} T + 12.05025 \quad (\text{XV:2})$$

Equation (XV:2) was selected since it represents a reasonable compromise among the known thermodynamic properties of cesium.

An alternate expression (ref. 19) for cesium vapor pressure based only on the various vapor pressure data (including recent work) is as follows:

$$\log_{10} p (\text{N/sq m}) = \frac{-3920.38}{T} - 0.519781 \log_{10} T + 10.71914 \quad (\text{XV:3})$$

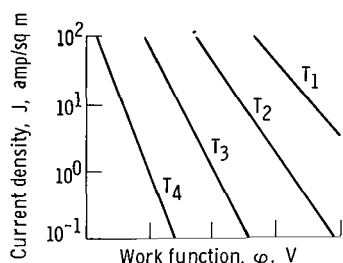


Figure XV:1. - Typical presentation of Richardson-Dushman equations.

Equation (XV:3), although in excellent agreement with experimental vapor pressure data (least-squares fit to the three-term expression), leads to incon-

TABLE XV:1. - COMPILED OF INTERCEPTS OF RICHARDSON-LUSHMAN EQUATION FOR USE IN PREPARING GRAPHICAL SOLUTIONS

Tempera-ture, °K	Current density, amp/sq m				Tempera-ture, °K	Current density, amp/sq m				Tempera-ture, °K	Current density, amp/sq m			
	10 ⁻³	10 ⁰	10 ³	10 ⁶		10 ⁻³	10 ⁰	10 ³	10 ⁶		10 ⁻³	10 ⁰	10 ³	10 ⁶
	Work function, eV					Work function, eV					Work function, eV			
500	1.436	1.139	0.541	0.543	1400	4.270	3.436	2.603	1.770	2300	5.842	4.473	3.104	
510	1.467	1.163	0.560	0.556	1410	4.302	3.463	2.623	1.784	2410	5.869	4.494	3.120	
520	1.497	1.188	0.578	0.569	1420	4.334	3.489	2.644	1.799	2420	5.896	4.516	3.135	
530	1.528	1.212	0.597	0.581	1430	4.366	3.515	2.665	1.813	2430	5.924	4.537	3.150	
540	1.558	1.237	0.715	0.594	1440	4.399	3.541	2.684	1.827	2440	5.951	4.558	3.165	
550	1.587	1.261	0.734	0.607	1450	4.431	3.568	2.705	1.842	2350	5.978	4.579	3.180	
560	1.619	1.286	0.953	0.619	1460	4.463	3.594	2.725	1.856	2360	6.005	4.600	3.196	
570	1.650	1.311	0.972	0.632	1470	4.495	3.620	2.746	1.871	2370	6.042	4.622	3.211	
580	1.681	1.336	0.990	0.645	1480	4.528	3.647	2.766	1.885	2380	6.059	4.643	3.226	
590	1.711	1.360	1.009	0.658	1490	4.560	3.673	2.786	1.900	2390	6.087	4.664	3.242	
600	1.742	1.385	1.028	0.671	1500	4.592	3.700	2.807	1.914	2400	6.114	4.685	3.257	
610	1.773	1.410	1.047	0.684	1510	4.625	3.722	2.827	1.929	2410	6.141	4.707	3.272	
620	1.804	1.435	1.066	0.697	1520	4.657	3.752	2.848	1.943	2420	6.168	4.728	3.287	
630	1.835	1.460	1.085	0.710	1530	4.689	3.779	2.868	1.958	2430	6.195	4.749	3.303	
640	1.865	1.485	1.104	0.723	1540	4.722	3.805	2.889	1.972	2440	6.223	4.770	3.318	
650	1.496	1.509	1.123	0.736	1550	4.754	3.832	2.909	1.987	2450	6.250	4.792	3.333	
660	1.497	1.534	1.142	0.749	1560	4.787	3.858	2.930	2.001	2460	6.277	4.813	3.349	
670	1.495	1.559	1.161	0.762	1570	4.819	3.885	2.950	2.016	2470	6.304	4.834	3.364	
680	1.789	1.984	1.180	0.775	1580	4.851	3.911	2.971	2.030	2480	6.332	4.855	3.379	
690	2.020	1.609	1.199	0.788	1590	4.884	3.938	2.991	2.045	2490	6.359	4.877	3.395	
700	2.051	1.635	1.218	0.801	1600	4.916	3.964	3.012	2.059	2500	6.386	4.898	3.410	
710	2.082	1.660	1.237	0.814	1610	4.949	3.991	3.032	2.074	2510	6.413	4.919	3.426	
720	2.113	1.685	1.256	0.828	1620	4.981	4.017	3.053	2.089	2520	6.441	4.941	3.441	
730	2.144	1.710	1.275	0.841	1630	5.014	4.044	3.073	2.103	2530	6.468	4.962	3.456	
740	2.175	1.735	1.295	0.854	1640	5.046	4.070	3.094	2.118	2540	6.495	4.983	3.472	
750	2.207	1.760	1.314	0.867	1650	5.079	4.097	3.115	2.133	2550	6.523	5.005	3.487	
760	2.238	1.785	1.333	0.881	1660	5.111	4.123	3.135	2.147	2560	6.550	5.026	3.502	
770	2.269	1.811	1.352	0.894	1670	5.144	4.150	3.156	2.162	2570	6.577	5.047	3.518	
780	2.300	1.836	1.372	0.907	1680	5.176	4.176	3.176	2.177	2580	6.604	5.069	3.533	
790	2.331	1.861	1.391	0.921	1690	5.209	4.203	3.197	2.191	2590	6.632	5.090	3.549	
800	2.363	1.886	1.410	0.934	1700	5.241	4.230	3.218	2.206	2600	6.659	5.112	3.564	
810	2.394	1.912	1.430	0.948	1710	5.274	4.256	3.238	2.221	2610	6.686	5.133	3.580	
820	2.423	1.937	1.449	0.961	1720	5.307	4.283	3.259	2.235	2620	6.714	5.154	3.595	
830	2.456	1.962	1.468	0.974	1730	5.339	4.309	3.280	2.250	2630	6.741	5.176	3.610	
840	2.488	1.988	1.488	0.988	1740	5.372	4.336	3.300	2.265	2640	6.768	5.197	3.626	
850	2.517	2.013	1.501	1.001	1750	5.404	4.363	3.321	2.280	2650	6.796	5.219	3.641	
860	2.551	2.039	1.527	1.015	1760	5.437	4.389	3.342	2.294	2660	6.823	5.240	3.657	
870	2.582	2.064	1.546	1.026	1770	5.470	4.416	3.363	2.309	2670	6.851	5.261	3.672	
880	2.613	2.090	1.561	1.042	1780	5.502	4.443	3.383	2.324	2680	6.878	5.283	3.688	
890	2.643	2.115	1.576	1.056	1790	5.535	4.469	3.404	2.339	2690	6.905	5.304	3.703	
900	2.676	2.141	1.605	1.069	1800	5.567	4.496	3.425	2.353	2700	6.933	5.326	3.719	
910	2.708	2.166	1.624	1.083	1810	5.600	4.523	3.445	2.368	2710	6.960	5.347	3.734	
920	2.739	2.192	1.644	1.096	1820	5.633	4.550	3.466	2.383	2720	6.988	5.369	3.750	
930	2.771	2.217	1.664	1.110	1830	5.665	4.576	3.487	2.398	2730	7.015	5.390	3.765	
940	2.802	2.243	1.683	1.124	1840	5.698	4.603	3.508	2.413	2740	7.042	5.412	3.781	
950	2.834	2.268	1.701	1.137	1850	5.731	4.630	3.529	2.428	2750	7.070	5.433	3.796	
960	2.869	2.294	1.723	1.151	1860	5.764	4.656	3.549	2.442	2760	7.097	5.455	3.812	
970	2.907	2.320	1.742	1.165	1870	5.796	4.683	3.570	2.457	2770	7.125	5.476	3.828	
980	2.948	2.345	1.762	1.179	1880	5.829	4.710	3.591	2.472	2780	7.152	5.498	3.843	
990	2.980	2.371	1.782	1.192	1890	5.862	4.737	3.612	2.487	2790	7.180	5.519	3.858	
1000	2.492	2.391	1.801	1.206	1900	5.894	4.764	3.633	2.502	2800	7.207	5.541	3.874	
1010	3.025	2.422	1.821	1.220	1910	5.927	4.790	3.654	2.517	2810	7.235	5.562	3.890	
1020	3.055	2.448	1.841	1.234	1920	5.960	4.817	3.674	2.532	2820	7.264	5.584	3.905	
1030	3.087	2.474	1.861	1.245	1930	5.993	4.844	3.695	2.547	2830	7.290	5.605	3.921	
1040	3.116	2.499	1.880	1.261	1940	6.025	4.871	3.716	2.561	2840	7.317	5.627	3.936	
1050	3.150	2.525	1.900	1.275	1950	6.058	4.898	3.737	2.576	2850	7.344	5.648	3.952	
1060	3.181	2.551	1.920	1.289	1960	6.091	4.924	3.758	2.591	2860	7.372	5.670	3.968	
1070	3.214	2.577	1.940	1.303	1970	6.124	4.951	3.779	2.606	2870	7.399	5.691	3.983	
1080	3.245	2.603	1.960	1.317	1980	6.157	4.978	3.800	2.621	2880	7.427	5.713	3.999	
1090	3.277	2.628	1.978	1.331	1990	6.190	5.005	3.821	2.636	2890	7.455	5.734	4.014	
1100	3.304	2.654	2.000	1.345	2000	6.222	5.032	3.842	2.651	2900	7.482	5.756	4.030	
1110	3.331	2.680	2.019	1.359	2010	6.255	5.059	3.863	2.666	2910	7.510	5.778	4.046	
1120	3.373	2.706	2.039	1.373	2020	6.288	5.086	3.883	2.681	2920	7.537	5.799	4.061	
1130	3.404	2.732	2.059	1.387	2030	6.321	5.113	3.904	2.696	2930	7.565	5.821	4.077	
1140	3.446	2.758	2.079	1.401	2040	6.354	5.140	3.925	2.711	2940	7.592	5.842	4.092	
1150	3.468	2.784	2.099	1.415	2050	6.387	5.166	3.946	2.726	2950	7.620	5.864	4.108	
1160	3.500	2.810	2.119	1.429	2060	6.420	5.193	3.967	2.741	2960	7.647	5.886	4.124	
1170	3.532	2.836	2.139	1.443	2070	6.452	5.220	3.988	2.756	2970	7.675	5.907	4.139	
1180	3.564	2.862	2.159	1.457	2080	6.485	5.247	4.009	2.771	2980	7.702	5.929	4.155	
1190	3.596	2.888	2.179	1.471	2090	6.518	5.274	4.030	2.786	2990	7.730	5.950	4.171	
1200	3.628	2.914	2.200	1.485	2100	6.551	5.301	4.051	2.801	3000	7.758	5.972	4.186	
1210	3.660	2.940	2.219	1.499	2110	6.584	5.328	4.072	2.816	3010	7.785	6.004	4.202	
1220	3.692	2.966	2.239	1.513	2120	6.617	5.355	4.093	2.832	3020	7.813	6.015	4.218	
1230	3.724	2.992	2.260	1.527	2130	6.650	5.382	4.114	2.847	3030	7.840	6.037	4.233	
1240	3.756	3.018	2.280	1.542	2140	6.683	5.409	4.135	2.862	3040	7.868	6.059	4.249	
1250	3.788	3.044	2.300	1.556	2150	6.716	5.436	4.156	2.877	3050	7.896	6.080	4.265	
1260	3.820	3.070	2.320	1.570	2160	6.749	5.463	4.178	2.892	3060	7.923	6.102	4.281</td	

TABLE XV.—RECOVERY OF CELLS AND VARIOUS PROTEINS IN BEANS

^aBond 22.0475±0.15

TABLE IV. 2. INDEX OF SUSPENDED SOLIDS IN THE RIVER

TABLE IV - CGC1 = VAPOR PRESSURE RELATION (BASED ON "BEST FIT" OF VAPOR PRESSURE DATA)

Temp., °K	Cooling vapor pressure, N/m²	Vapor density, atoms/cm³	Mean free path, m	Evap. rate, kg/m²/s	Atom arrival time, sec.	Ten- pera- ture, °K	Cooling vapor pres- sure, N/m²	Vapor density, atoms/cm³	Mean free path, m	Evap. rate, kg/m²/s	Atom arrival time, sec.		
250	6.61827 × 10⁻⁶	4.63068 × 10⁻¹	17912.35	11407.8	59912.16	16322.7	400	36782.0	27356.2	66505.20	37979.2	42049.22	67366.9
251	7.12151	5.3431	20259.1	12291.1	10281.17	1867.2	401	38861.0	29187.7	70191.0	35959.2	44271.1	71056.1
252	7.62420	5.8750	22659.1	13559.1	11551.17	21712.0	402	41231.0	30365.7	72019.0	36354.2	45364.1	72086.1
253	8.12722	6.3159	26595.1	19361.3	13551.2	21712.0	403	43392.0	32504.0	77905.0	32234.1	45364.1	70086.1
254	8.63077	6.7010	30695.1	23056.3	13551.2	21712.0	404	45754.0	34313.7	82036.0	30801.1	52076.1	83392.1
255	9.13421	7.0877	35081.1	28597.3	13552.2	21712.0	405	48117.0	36322.7	82036.0	30801.1	52076.1	83392.1
256	9.63765	7.4744	40595.1	35251.3	13553.2	21712.0	406	50480.0	38332.7	82036.0	30801.1	52076.1	83392.1
257	10.14109	7.8611	47976.1	43729.3	13554.2	21712.0	407	52853.0	40343.7	82036.0	30801.1	52076.1	83392.1
258	10.64453	8.2478	54592.1	50426.3	13555.2	21712.0	408	55226.0	42353.7	82036.0	30801.1	52076.1	83392.1
259	11.14797	8.6345	62010.1	56571.3	13556.2	21712.0	409	57597.0	44363.7	82036.0	30801.1	52076.1	83392.1
260	11.65141	9.0212	70428.1	62724.3	13557.2	21712.0	410	60960.0	46373.7	82036.0	30801.1	52076.1	83392.1
261	12.15485	9.4079	76957.1	68288.3	13558.2	21712.0	411	63347.0	48383.7	82036.0	30801.1	52076.1	83392.1
262	12.65829	9.7946	83385.1	74022.3	13559.2	21712.0	412	65724.0	50393.7	82036.0	30801.1	52076.1	83392.1
263	13.16173	10.1813	90813.1	80561.3	13560.2	21712.0	413	68101.0	52403.7	82036.0	30801.1	52076.1	83392.1
264	13.66517	10.5680	98241.1	86295.3	13561.2	21712.0	414	70478.0	54413.7	82036.0	30801.1	52076.1	83392.1
265	14.16861	10.9547	105669.1	91986.3	13562.2	21712.0	415	72856.0	56423.7	82036.0	30801.1	52076.1	83392.1
266	14.67205	11.3414	113107.1	98664.3	13563.2	21712.0	416	75233.0	58433.7	82036.0	30801.1	52076.1	83392.1
267	15.17549	11.7281	120545.1	105294.3	13564.2	21712.0	417	77610.0	60443.7	82036.0	30801.1	52076.1	83392.1
268	15.67893	12.1148	128983.1	111951.3	13565.2	21712.0	418	80987.0	62453.7	82036.0	30801.1	52076.1	83392.1
269	16.18237	12.5015	137421.1	118619.3	13566.2	21712.0	419	83364.0	64463.7	82036.0	30801.1	52076.1	83392.1
270	16.68581	12.8882	145859.1	125247.3	13567.2	21712.0	420	85741.0	66473.7	82036.0	30801.1	52076.1	83392.1
271	17.18925	13.2749	154297.1	131935.3	13568.2	21712.0	421	88118.0	68483.7	82036.0	30801.1	52076.1	83392.1
272	17.69269	13.6626	162735.1	138602.3	13569.2	21712.0	422	90495.0	70493.7	82036.0	30801.1	52076.1	83392.1
273	18.19613	14.0503	171173.1	145269.3	13570.2	21712.0	423	92872.0	72503.7	82036.0	30801.1	52076.1	83392.1
274	18.69957	14.4380	179611.1	152040.3	13571.2	21712.0	424	95249.0	74513.7	82036.0	30801.1	52076.1	83392.1
275	19.19301	14.8257	188050.1	159664.3	13572.2	21712.0	425	97626.0	76523.7	82036.0	30801.1	52076.1	83392.1
276	19.69645	15.2124	196488.1	167291.3	13573.2	21712.0	426	100003.0	78533.7	82036.0	30801.1	52076.1	83392.1
277	20.19989	15.5991	204926.1	173958.3	13574.2	21712.0	427	10238.0	80543.7	82036.0	30801.1	52076.1	83392.1
278	20.69333	16.0868	213364.1	181675.3	13575.2	21712.0	428	10475.0	82553.7	82036.0	30801.1	52076.1	83392.1
279	21.19677	16.4745	221802.1	189392.3	13576.2	21712.0	429	10712.0	84563.7	82036.0	30801.1	52076.1	83392.1
280	21.69021	16.8622	230240.1	197119.3	13577.2	21712.0	430	10949.0	86573.7	82036.0	30801.1	52076.1	83392.1
281	22.18365	17.2499	238678.1	204836.3	13578.2	21712.0	431	11186.0	88583.7	82036.0	30801.1	52076.1	83392.1
282	22.67709	17.6376	247116.1	212563.3	13579.2	21712.0	432	11423.0	90593.7	82036.0	30801.1	52076.1	83392.1
283	23.17053	18.0253	255554.1	220900.3	13580.2	21712.0	433	11660.0	92503.7	82036.0	30801.1	52076.1	83392.1
284	23.66397	18.4130	263992.1	229227.3	13581.2	21712.0	434	11897.0	94513.7	82036.0	30801.1	52076.1	83392.1
285	24.15741	18.7997	272430.1	237564.3	13582.2	21712.0	435	12134.0	96523.7	82036.0	30801.1	52076.1	83392.1
286	24.65085	19.1874	280868.1	245897.3	13583.2	21712.0	436	12371.0	98533.7	82036.0	30801.1	52076.1	83392.1
287	25.14429	19.5751	289306.1	254226.3	13584.2	21712.0	437	12608.0	100543.7	82036.0	30801.1	52076.1	83392.1
288	25.63773	19.9628	297744.1	262655.3	13585.2	21712.0	438	12845.0	102553.7	82036.0	30801.1	52076.1	83392.1
289	26.13117	20.3505	306182.1	271084.3	13586.2	21712.0	439	13082.0	104563.7	82036.0	30801.1	52076.1	83392.1
290	26.62461	20.7382	314620.1	279513.3	13587.2	21712.0	440	13319.0	106573.7	82036.0	30801.1	52076.1	83392.1
291	27.11805	21.1259	323058.1	287942.3	13588.2	21712.0	441	13556.0	108583.7	82036.0	30801.1	52076.1	83392.1
292	27.61149	21.5136	331496.1	296371.3	13589.2	21712.0	442	13793.0	110593.7	82036.0	30801.1	52076.1	83392.1
293	28.10493	21.8913	340934.1	304799.3	13590.2	21712.0	443	14030.0	112603.7	82036.0	30801.1	52076.1	83392.1
294	28.59837	22.2790	349372.1	313232.3	13591.2	21712.0	444	14267.0	114613.7	82036.0	30801.1	52076.1	83392.1
295	29.09181	22.6667	357810.1	321665.3	13592.2	21712.0	445	14504.0	116623.7	82036.0	30801.1	52076.1	83392.1
296	29.58525	23.0544	366248.1	330198.3	13593.2	21712.0	446	14741.0	118633.7	82036.0	30801.1	52076.1	83392.1
297	30.07869	23.4421	374686.1	338631.3	13594.2	21712.0	447	15078.0	120643.7	82036.0	30801.1	52076.1	83392.1
298	30.57213	23.8298	383124.1	347064.3	13595.2	21712.0	448	15315.0	122653.7	82036.0	30801.1	52076.1	83392.1
299	31.06557	24.2175	391562.1	355497.3	13596.2	21712.0	449	15552.0	124663.7	82036.0	30801.1	52076.1	83392.1
300	31.55901	24.6052	400000.1	364930.3	13597.2	21712.0	450	15789.0	126673.7	82036.0	30801.1	52076.1	83392.1
301	32.05245	25.0029	408438.1	373363.3	13598.2	21712.0	451	16026.0	128683.7	82036.0	30801.1	52076.1	83392.1
302	32.54589	25.3906	416876.1	381796.3	13599.2	21712.0	452	16263.0	130693.7	82036.0	30801.1	52076.1	83392.1
303	33.03933	25.7783	425314.1	390229.3	13600.2	21712.0	453	16500.0	132703.7	82036.0	30801.1	52076.1	83392.1
304	33.53277	26.1660	433752.1	398662.3	13601.2	21712.0	454	16737.0	134713.7	82036.0	30801.1	52076.1	83392.1
305	34.02621	26.5537	442190.1	407095.3	13602.2	21712.0	455	17074.0	136723.7	82036.0	30801.1	52076.1	83392.1
306	34.51965	26.9414	450628.1	415528.3	13603.2	21712.0	456	17311.0	138733.7	82036.0	30801.1	52076.1	83392.1
307	35.01309	27.3291	459066.1	423957.3	13604.2	21712.0	457	17548.0	140743.7	82036.0	30801.1	52076.1	83392.1
308	35.50653	27.7168	467504.1	432386.3	13605.2	21712.0	458	17785.0	142753.7	82036.0	30801.1	52076.1	83392.1
309	35.99997	28.1045	475942.1	440815.3	13606.2	21712.0	459	18022.0	144763.7	82036.0	30801.1	52076.1	83392.1
310	36.49341	28.4922	484380.1	449244.3	13607.2	21712.0	460	18259.0	146773.7	82036.0	30801.1	52076.1	83392.1
311	36.98685	28.8799	492818.1	457673.3	13608.2	21712.0	461	18496.0	148783.7	82036.0	30801.1	52076.1	83392.1
312	37.48029	29.2676	501256.1	466102.3	13609.2	21712.0	462	18733.0	150793.7	82036.0	30801.1	52076.1	83392.1
313	37.97373	29.6553	509694.1	474531.3	13610.2	21712.0	463	19070.0	152803.7	82036.0	30801.1	52076.1	83392.1
314	38.46717	30.0430	518132.1	482960.3	13611.2	21712.0	464	19307.0	154813.7	82036.0	30801.1	52076.1	83392.1
315	38.96061	30.4277	526570.1	491389.3	13612.2	21712.0	465	19544.0	156823.7	82036.0	30801.1	52076.1	83392.1
316	39.45405	30.8154	535008.1	500815.3	13613.2	21712.0	466	19781.0	158833.7	82036.0	30801.1	52076.1	83392.1
317	39.94749	31.1931	543446.1	509									

TABLE XVII. - Concluded. EQUATION OF STATE RELATIONS (BASED ON "BEST FIT" OF VAPOR PRESSURE DATA)

Temperature, °K	Vapour pressure		Mean free path, cm	Collision rate, sec⁻¹	Atom arrival rate, sec⁻¹	Vapour pressure		Mean free path, cm	Collision rate, sec⁻¹	Arrival rate, sec⁻¹
	N/m²	Torr				[sq cm/sec]	[sq cm/sec]			
550	-1.6681	1	+1.1111	-1.2335	23	+1.0269	-1.0112	25	+2.0710	6
551	-1.5110	1	+1.1553	-1.0865	22	+1.2772	-1.1718	25	+2.0710	6
552	-1.4551	1	+1.2023	-1.2367	22	+1.1519	-1.2453	25	+2.0710	6
553	-1.4022	1	+1.2053	-1.2062	22	+1.1519	-1.2453	25	+2.0710	6
554	-6.6465	1	+1.2550	-2.1529	11737	+1.9993	-2.0425	704	+6.802	35105
555	-6.6940	3	+1.2705	-1.2110	23	+1.0229	-1.0444	25	+2.0539	6
556	-1.5723	1	+1.1553	-1.0865	22	+1.2772	-1.1718	25	+2.0710	6
557	-1.7925	1	+1.3445	-2.3312	10859	+1.7966	-2.7821	703	+5.1712	20518
558	-1.7436	1	+1.3445	-2.3312	10858	+1.7965	-2.7820	703	+5.1712	20517
559	-1.8940	1	+1.2221	-1.2549	22	+1.1519	-1.2453	25	+2.0710	6
560	-1.9487	1	+1.6262	-1.5220	23	+1.0219	-1.0445	25	+2.0538	6
561	-2.0047	1	+1.5163	-2.5986	9.9762	+1.9152	-2.1002	703	+5.1229	15390
562	-2.0587	1	+1.5163	-2.5986	9.9762	+1.9152	-2.1002	703	+5.1229	15389
563	-2.1187	1	+1.5901	-2.7259	2.9266	+2.0116	-2.3707	703	+5.1229	15387
564	-2.1777	1	+1.6354	-2.9770	70741	+2.0961	-2.5589	704	+5.6040	41705
565	-2.2383	1	+1.6781	-3.1606	2.9055	+2.1532	-2.6492	704	+5.6051	42416
566	-2.2977	1	+1.7225	-3.3436	2.9055	+2.1532	-2.6492	704	+5.6051	42415
567	-2.3537	1	+1.7225	-3.3437	2.9056	+2.1532	-2.6492	704	+5.6051	42416
568	-2.4120	1	+1.7653	-3.5243	2.9056	+2.1532	-2.6492	704	+5.6051	42415
569	-2.4693	1	+1.7653	-3.5243	2.9056	+2.1532	-2.6492	704	+5.6051	42415
570	-2.5262	3	+1.8225	-1	+1.2576	-23	+1.1522	-25	+2.0537	6
571	-2.6029	1	+1.7401	-2.7651	25	+2.0537	-2.6193	6	+2.0537	6
572	-2.6542	1	+1.7401	-2.7651	25	+2.0537	-2.6193	6	+2.0537	6
573	-2.7172	1	+2.0831	-3.1109	7.9191	+2.5257	-2.4248	703	+5.6040	36055
574	-2.8519	1	+2.0831	-3.1109	7.9191	+2.5257	-2.4248	703	+5.6040	36054
575	-2.9183	1	+2.1964	-3	+1.6891	-25	+1.0473	-22	+2.0524	6
576	-3.0730	1	+2.1964	-3	+1.6891	-25	+1.0473	-22	+2.0524	6
577	-3.1255	1	+2.1964	-3	+1.6891	-25	+1.0473	-22	+2.0524	6
578	-3.1777	1	+2.1964	-3	+1.6891	-25	+1.0473	-22	+2.0524	6
579	-3.2291	1	+2.1964	-3	+1.6891	-25	+1.0473	-22	+2.0524	6
580	-3.3317	3	+2.1964	-1	+1.6891	-23	+1.0473	-22	+2.0524	6
581	-3.6152	1	+2.0591	-2.7705	32491	+2.0592	-2.7705	703	+5.6040	15031
582	-3.6672	1	+2.0591	-2.7705	32491	+2.0592	-2.7705	703	+5.6040	15030
583	-3.7202	1	+2.0591	-2.7705	32491	+2.0592	-2.7705	703	+5.6040	15029
584	-3.7699	1	+2.0591	-2.7705	32491	+2.0592	-2.7705	703	+5.6040	15028
585	-3.8223	1	+2.0591	-2.7705	32491	+2.0592	-2.7705	703	+5.6040	15027
586	-3.8748	1	+2.0591	-2.7705	32491	+2.0592	-2.7705	703	+5.6040	15026
587	-3.9273	1	+2.0591	-2.7705	32491	+2.0592	-2.7705	703	+5.6040	15025
588	-3.9798	1	+2.0591	-2.7705	32491	+2.0592	-2.7705	703	+5.6040	15024
589	-4.0323	1	+2.0591	-2.7705	32491	+2.0592	-2.7705	703	+5.6040	15023
590	-4.0848	3	+2.0591	-1	+1.6891	-23	+1.0473	-22	+2.0524	6
591	-4.1373	1	+2.0591	-1	+1.6891	-23	+1.0473	-22	+2.0524	6
592	-4.1898	1	+2.0591	-1	+1.6891	-23	+1.0473	-22	+2.0524	6
593	-4.2423	1	+2.0591	-1	+1.6891	-23	+1.0473	-22	+2.0524	6
594	-4.2948	1	+2.0591	-1	+1.6891	-23	+1.0473	-22	+2.0524	6
595	-4.3473	1	+2.0591	-1	+1.6891	-23	+1.0473	-22	+2.0524	6
596	-4.3998	1	+2.0591	-1	+1.6891	-23	+1.0473	-22	+2.0524	6
597	-4.4523	1	+2.0591	-1	+1.6891	-23	+1.0473	-22	+2.0524	6
598	-4.5048	1	+2.0591	-1	+1.6891	-23	+1.0473	-22	+2.0524	6
599	-4.5573	1	+2.0591	-1	+1.6891	-23	+1.0473	-22	+2.0524	6
600	-4.6108	3	+2.0591	-1	+1.6891	-23	+1.0473	-22	+2.0524	6
601	-4.6633	1	+2.0591	-1	+1.6891	-23	+1.0473	-22	+2.0524	6
602	-4.7158	1	+2.0591	-1	+1.6891	-23	+1.0473	-22	+2.0524	6
603	-4.7683	1	+2.0591	-1	+1.6891	-23	+1.0473	-22	+2.0524	6
604	-4.8208	1	+2.0591	-1	+1.6891	-23	+1.0473	-22	+2.0524	6
605	-4.8733	1	+2.0591	-1	+1.6891	-23	+1.0473	-22	+2.0524	6
606	-4.9258	1	+2.0591	-1	+1.6891	-23	+1.0473	-22	+2.0524	6
607	-4.9783	1	+2.0591	-1	+1.6891	-23	+1.0473	-22	+2.0524	6
608	-5.0308	1	+2.0591	-1	+1.6891	-23	+1.0473	-22	+2.0524	6
609	-5.0833	1	+2.0591	-1	+1.6891	-23	+1.0473	-22	+2.0524	6
610	-5.1358	1	+2.0591	-1	+1.6891	-23	+1.0473	-22	+2.0524	6
611	-5.1883	1	+2.0591	-1	+1.6891	-23	+1.0473	-22	+2.0524	6
612	-5.2408	1	+2.0591	-1	+1.6891	-23	+1.0473	-22	+2.0524	6
613	-5.2933	1	+2.0591	-1	+1.6891	-23	+1.0473	-22	+2.0524	6
614	-5.3458	1	+2.0591	-1	+1.6891	-23	+1.0473	-22	+2.0524	6
615	-5.3983	1	+2.0591	-1	+1.6891	-23	+1.0473	-22	+2.0524	6
616	-5.4508	1	+2.0591	-1	+1.6891	-23	+1.0473	-22	+2.0524	6
617	-5.5033	1	+2.0591	-1	+1.6891	-23	+1.0473	-22	+2.0524	6
618	-5.5558	1	+2.0591	-1	+1.6891	-23	+1.0473	-22	+2.0524	6
619	-5.6083	1	+2.0591	-1	+1.6891	-23	+1.0473	-22	+2.0524	6
620	-5.6608	3	+2.0591	-1	+1.6891	-23	+1.0473	-22	+2.0524	6
621	-5.7133	1	+2.0591	-1	+1.6891	-23	+1.0473	-22	+2.0524	6
622	-5.7658	1	+2.0591	-1	+1.6891	-23	+1.0473	-22	+2.0524	6
623	-5.8183	1	+2.0591	-1	+1.6891	-23	+1.0473	-22	+2.0524	6
624	-5.8708	1	+2.0591	-1	+1.6891	-23	+1.0473	-22	+2.0524	6
625	-5.9233	1	+2.0591	-1	+1.6891	-23	+1.0473	-22	+2.0524	6
626	-5.9758	1	+2.0591	-1	+1.6891	-23	+1.0473	-22	+2.0524	6
627	-6.0283	1	+2.0591	-1	+1.6891	-23	+1.0473	-22	+2.0524	6
628	-6.0808	1	+2.0591	-1	+1.6891	-23	+1.0473	-22	+2.0524	6
629	-6.1333	1	+2.0591	-1	+1.6891	-23	+1.0473	-22	+2.0524	6
630	-6.1858	1	+2.0591	-1	+1.6891	-23	+1.0473	-22	+2.0524	6
631	-6.2383	1	+2.0591	-1	+1.6891	-23	+1.0473	-22	+2.0524	6
632	-6.2908	1	+2.0591	-1	+1.6891	-23	+1.0473	-22	+2.0524	6
633	-6.3433	1	+2.0591	-1	+1.6891	-23	+1.0473	-22	+2.0524	6
634	-6.3958	1	+2.0591	-1	+1.6891	-23	+1.0473	-22	+2.0524	6
635	-6.4483	1	+2.0591	-1	+1.6891	-23	+1.0473	-22	+2.0524	6
636	-6.4998	1	+2.0591	-1	+1.6891	-23	+1.0473	-22	+2.0524	6
637	-6.5523	1	+2.0591	-1	+1.6891	-23	+1.0473	-22	+2.0524	6
638	-6.6048	1	+2.0591	-1	+1.6891	-23	+1.0473	-22	+2.0524	6
639	-6.6573	1	+2.0591	-1	+1.6891	-23	+1.0473	-22	+2.0524	6
640	-6.7198	1	+2.0591	-1	+1.6891	-23	+1.0473	-22	+2.0524	6
641	-6.7723	1	+2.0591	-1	+1.6891	-23	+1.0473	-22	+2.0524	6
642	-6.8248	1	+2.0591	-1	+1.6891	-23	+1.0473	-22	+2.0524	6
643	-6.8773	1	+2.0591	-1	+1.6891	-23	+1.0473	-22	+2.0524	6
644	-6.9308	1	+2.0591	-1	+1.6891	-23	+1.0473	-22	+2.0524	6
645	-6.9833	1	+2.0591	-1	+1.6891	-23	+1.0473	-22	+2.0524	6
646	-7.0358	1	+2.0591	-1	+1.6891	-23	+1.0473	-22	+2.0524	6
647	-7.0883	1	+2.0591	-1	+1.6891	-23	+1.0473	-22	+2.0524	6
648	-7.1408	1	+2.0591	-1	+1.6891	-23	+1.0473	-22	+2.0524	6
649	-7.1933	1	+2.0591	-1	+1.6891	-23	+1.0473	-22	+2.0524	6
650	-7.2458	1	+2.0591	-1	+1.6891	-23	+1.0473	-22	+2.0524	6
651	-7.2983	1	+2.0591	-1	+1.6891	-23	+1.0473	-22	+2.0524	6
652	-7.3508	1	+2.0591	-1	+1.6891	-23	+1.0473	-22	+2.0524	6
653	-7.4033	1	+2.0591	-1	+1.6891	-23	+1.0473	-22	+2.0524	6
654	-7.4558	1	+2.0591	-1	+1.6891	-23	+1.0473	-22	+2.0524	6
655	-7.5083	1	+2.0591	-1	+1.6891	-23	+1.0473	-22	+2.0524	6
656	-7.5608	1	+2.0591	-1	+1.6891	-23	+1.0473	-22	+2.0524	6
657	-7.6133	1	+2.0591	-1	+1.6891	-23	+1.0473	-22	+2.0524	6
658	-7.6658	1	+2.0591	-1	+1.6891	-23	+1.0473	-22	+2.0524	6
659	-7.7183	1	+2.0591	-1	+1.6891					

sistencies in the heat of condensation of the monomer at 0° K. Tabulated values of the two vapor pressure relations are given in tables XV:2 and XV:3. Table XV:2 is the table recommended because of its thermodynamic self consistency. Table XV:3 is included as a concession to those who wish to emphasize vapor pressure data alone. The values given in table XV:3 are more consistent with those used in past thermionic research.

Included in the tables are related quantities of interest, namely, particle density, mean free path for electron-neutral collisions, and atom flux rate in terms of particles per square meter per second and in terms of an equivalent atom current density (atom flux divided by 6.24×10^{18}). The cross section used for the electron-neutral interaction corresponds to a reciprocal mean free path at standard conditions ($P_c = 1400 \text{ cm}^{-1}$).

The aforementioned tables, being based on equilibrium liquid-vapor pressure measurements, must be modified for use at the conditions existent in the thermionic converter. Exact relations that describe the various properties are complex because of the many possible interactions that occur in the plasma.

A useful approximate relation is derivable from kinetic theory for use in the free molecule flow range. The result expressed in terms of a temperature multiplying factor R_T is

$$R_T = \frac{\sqrt{T_2 T_{Cs}} + \sqrt{T_1 T_{Cs}}}{2\sqrt{T_1 T_2}} \quad (\text{XV:4})$$

$$n(\text{interelectrode}) = R_T n_{Cs} \quad (\text{XV:5})$$

$$\lambda(\text{interelectrode}) = \frac{\lambda_{Cs}}{R_T} \quad (\text{XV:6})$$

where the subscript Cs refers to measurements of the vapor in equilibrium with the liquid. The flux equations to emitter and collector surface are unaltered since free molecular flow is assumed.

Similar correction factors for the continuum condition of constant pressure can be obtained. From the perfect gas law, there results

$$n = n_{Cs} \frac{T_{Cs}}{T_1} \quad (\text{XV:7})$$

$$\lambda = \frac{T_1}{T_{Cs}} \lambda_{Cs} \quad (\text{XV:8})$$

$$v = v_{Cs} \sqrt{\frac{T_{Cs}}{T}} \quad (\text{XV:9})$$

The transition between free molecule and continuum can be established by the extensions of the previous approach but are of questionable use because the unknowns related to plasma effects would probably mask these corrections. It should be noted that in many cases corrections due to poor conductance between the cesium reservoir and the interelectrode space introduce additional corrections of the nature illustrated previously.

XVI - CONCLUDING REMARKS

Thermionic converters cannot be constructed or analyzed in detail by the simple theories outlined in the preceding sections. Greater attention to the various complex interactions is required to achieve these ends; however, a very significant step can be achieved in the general understanding of the mechanisms at play in practical converters by the approaches outlined. The point of view used in each section was to emphasize or develop simple relations directly derivable from existent theory. Simplicity was emphasized because of the subsequent utility of the resulting equations, tables, or figures in treating experimental data. No new theories or analyses have been advanced. An attempt has been made to clarify, combine, compile, and suggest how to use theories and relations that are the basic foundation of thermionic converter analyses. The cesium-filled thermionic converter has been emphasized, and many of the relations were numerically evaluated for cesium because of the great promise of a cesium-filled converter. Nonetheless, the results presented are equally applicable to other systems with appropriate adjustments of physical constants.

XVII - SYMBOLS

E	field strength, V/m
f	fractional ionization
<i>f</i>	function
h	Planck's constant, 6.6242×10^{-34} , J-sec
I _F	Schottky enhanced emission current, amp
I ₀	saturation emission current, amp
J	current density, amp/sq m
-J _B	electron current density at arbitrary applied voltage V _B , amp/sq m
J _{MBL}	current density at the Maxwell-Boltzmann limit (zero field at collector), amp/sq m
+J _p	random ion current density in isothermal plasma, amp/sq m

$-J_p$	random electron current density in isothermal plasma, amp/sq m
J_0	saturation emission current density (zero field at emitter) amp/sq m
$-J_0$	electron saturation emission current density (zero field at emitter), amp/sq m
K	constant used in dimensionless distance parameter of space-charge relations, $(^{\circ}\text{K})^{3/4}/\text{amp}^{1/2}$
k	Boltzmann's constant, $1.3805 \times 10^{-23} \text{ J}/^{\circ}\text{K}$
m	particle mass, kg
n	particle concentration, particles/cu m
n_{Cs}	cesium atom concentration, atom/cu m
$+n_p$	cesium ion concentration, ion/cu m
$-n_p$	electron concentration, electrons/cu m
P	probability integral, $P(\psi^{1/2}) = \frac{2}{\sqrt{\pi}} \int_0^y e^{-y^2} dy$
P_c	cross section parameter, cm ⁻¹
p	pressure, N/sq m
q	electron charge, $1.602 \times 10^{-19} \text{ C}$
R_T	temperature ratio
S	slope of Schottky plot (eq. IX:14)
T	temperature, $^{\circ}\text{K}$
T_{Cs}	temperature of liquid cesium reservoir, $^{\circ}\text{K}$
T_1	temperature of emitter, $^{\circ}\text{K}$
T_2	temperature of collector, $^{\circ}\text{K}$
V	potential difference, V
V_B	potential difference between Fermi level of collector and Fermi level of emitter, V
V_C	contact potential difference between emitter and collector, V

V_i	ionization potential of cesium, V
V_{MBL}	potential difference between emitter and collector surfaces at Maxwell-Boltzmann limit, V
V_x	potential difference relative to isothermal plasma potential, V
w	distance between emitter and collector, m
w_{eff}	effective distance between emitter and collector resulting from constant field assumption
x	distance, m
x_M	distance from minimum space-charge barrier to emitter surface (in emitter space), m
x_N	distance from minimum space-charge barrier to collector surface (in collector space), m
$x_{\bar{V}}$	distance at which potential is equal to kT/q in Fowler sheath analysis, m
x_0	distance from real to fictitious surface in Fowler sheath analysis, m
x_1	distance parameter used in Fowler sheath analysis, $5/\sqrt{10^6}$ Debye lengths
ϵ_0	permittivity of free space, $8.85 \times 10^{-12} C^2/(N)(sq\ m)$
λ	mean free path, m
λ_{Cs}	mean free path at T_{Cs} , m
μ	isothermal plasma potential referenced to Fermi level, V
ν	particle flux density, particles/(sq m)(sec)
ν_{Cs}	particle flux density at T_{Cs} , particles/(sq m)(sec)
ϕ	work function, V
ϕ_{MBL}	barrier potential referenced to emitter Fermi level at Maxwell-Boltzmann limit, V
ϕ_1	emitter work function, V
ϕ_2	collector work function, V
χ	dimensionless distance, $KJ^{1/2}x/T^{3/4}$
χ_c	dimensionless distance in collector space (see fig. III:1)

$x_{C,N}$	dimensionless distance corresponding to x_N
$x_{C,0}$	dimensionless distance corresponding to zero field at emitter (saturated current)
x_E	dimensionless distance in emitter space
$x_{E,M}$	dimensionless distance corresponding to x_M
$x_{E,MBL}$	dimensionless distance corresponding to zero field at collector (MBL)
ψ	dimensionless potential, qV/kT
ψ_C	dimensionless potential in collector space
$\psi_{C,N}$	dimensionless potential corresponding to x_N
$\psi_{C,0}$	dimensionless potential corresponding to zero field at emitter (saturated current)
ψ_E	dimensionless potential in emitter space
$\psi_{E,M}$	dimensionless potential corresponding to x_M
$\psi_{E,MBL}$	dimensionless potential corresponding to zero field at collector (MBL)
ψ_1	dimensionless potential $(\phi_1 - \mu)/(kT/q)$ used in Fowler theory

Lewis Research Center,
 National Aeronautics and Space Administration,
 Cleveland, Ohio, October 26, 1965.

XVIII - REFERENCES

1. Langmuir, I.: The Effect of Space Charge and Initial Velocities on the Potential Distribution and Thermionic Current Between Parallel Plane Electrodes. *Phys. Rev.*, vol. 21, Apr. 1923, pp. 419-435.
2. Nottingham, W. B.: Thermionic Emission. Rept. No. TR-321, M.I.T., Dec. 10, 1956.
3. Poritsky, H.: Electron Gas Equations for Electric Flow in Diodes. *IRE Trans. Prof. Group on Electron Devices PGE-2*, Jan. 1953, pp. 60-84.
4. Kleijnen, P.H.J.A.: Extension of Langmuir's (χ , η) Tables for Plane Diode with Maxwellian Distribution of Electrons. *Phillips Res. Rev.*, vol. 1, no. 2, Jan. 1946, pp. 81-96.

5. Ferris, W. R.: Some Characteristics of Diodes with Oxide-Coated Cathodes. RCA Rev., vol. 10, no. 1, Mar. 1949, pp. 134-149.
6. Schottky, Walter: Über den Austritt von Elektronen aus Glühderähten bei Verzogernden Potentialen. Ann. Physik, vol. 44, 1914, pp. 1011-1032.
7. Morris, James F.: Thermal Field Emission with a Terminated Image Potential. NASA TN D-2784, 1965.
8. Langmuir, I.: Nature of Adsorbed Films of Caesium on Tungsten. Phys. Rev., vol. 43, no. 4, Feb. 15, 1933, pp. 224-251.
9. Taylor, J. B.; and Langmuir, I.: Evaporation of Atoms, Ions and Electrons from Caesium Films on Tungsten. Phys. Rev., vol. 44, Sept. 1933, pp. 423-458.
10. Breitwieser, Roland: On the Relation of Ion and Electron Emission to Diode Diagnostics. Inst. Elec. and Electron. on Thermionic Conversion Specialists Conf., Oct. 7-9, 1963, pp. 17-26.
11. Nottingham, Wayne B.: Sheath and Plasma Theory of an Isothermal Diode. Rept. No. 4-62, Thermo Electron Eng. Corp., Oct. 1962.
12. Saha, M. N.: Ionization in the Solar Chromosphere. Phil. Mag., vol. 40, Oct. 1920, pp. 472-488.
13. Mayer, J. E.; and Mayer, M. G.: Statistical Mechanics. John Wiley & Sons, Inc., 1959.
14. Fowler, R. H.: The Restored Electron Theory of Metals and Thermionic Formulas. Proc. Roy. Soc. (London), ser. A, vol. 117, 1928, pp. 549-552.
15. Houston, John M.: Ion Current in the Retarding-Range Cesium Thermionic Converter. Rept. on Twenty-Fourth Conf. on Phys. Electronics, M.I.T., Mar. 25-27, 1964, pp. 211-223.
16. Luke, Keung P.; and Smith, John R.: Theoretical Study of Zero-Field Electron Work Function of Metal Immersed in Gas-Direct Application of Cesium Thermionic Diode. NASA TN D-2357, 1964.
17. Nottingham, W. B.: Cesium Plasma Diode as a Heat-to-Electrical-Power Transducer. Direct Conversion of Heat to Electricity, J. Kaye and J. A. Welsh, eds., John Wiley & Sons, Inc., 1960, pp. 8-1 - 8-37.
18. Honig, R. E.: Vapor Pressure Data for Solid and Liquid Elements. RCA Rev., vol. 23, no. 4, Dec. 1962, pp. 567-586.
19. Heimel, Sheldon: Thermodynamic Properties of Cesium up to 1500° K. NASA TN D-2906, 1965.

"The aeronautical and space activities of the United States shall be conducted so as to contribute . . . to the expansion of human knowledge of phenomena in the atmosphere and space. The Administration shall provide for the widest practicable and appropriate dissemination of information concerning its activities and the results thereof."

—NATIONAL AERONAUTICS AND SPACE ACT OF 1958

NASA SCIENTIFIC AND TECHNICAL PUBLICATIONS

TECHNICAL REPORTS: Scientific and technical information considered important, complete, and a lasting contribution to existing knowledge.

TECHNICAL NOTES: Information less broad in scope but nevertheless of importance as a contribution to existing knowledge.

TECHNICAL MEMORANDUMS: Information receiving limited distribution because of preliminary data, security classification, or other reasons.

CONTRACTOR REPORTS: Technical information generated in connection with a NASA contract or grant and released under NASA auspices.

TECHNICAL TRANSLATIONS: Information published in a foreign language considered to merit NASA distribution in English.

TECHNICAL REPRINTS: Information derived from NASA activities and initially published in the form of journal articles.

SPECIAL PUBLICATIONS: Information derived from or of value to NASA activities but not necessarily reporting the results of individual NASA-programmed scientific efforts. Publications include conference proceedings, monographs, data compilations, handbooks, sourcebooks, and special bibliographies.

Details on the availability of these publications may be obtained from:

SCIENTIFIC AND TECHNICAL INFORMATION DIVISION

NATIONAL AERONAUTICS AND SPACE ADMINISTRATION

Washington, D.C. 20546